C-H Activation by Ozone in Liquid CO_2 Using Cyclohexane and Iso-octane as Substrates

Xuhui Chen

B.E., Harbin Institute of Technology, 2016

Submitted to the graduate degree program in Chemical & Petroleum Engineering and the Graduate Faculty of the University of Kansas in partial fulfillment of the requirements for the degree of Master of Science.

Committee Members:

_____

Chair: Bala Subramaniam

_____

Raghunath V. Chaudhari

_____

Timothy Jackson

Date Defended: August 29, 2018

The thesis committee for Xuhui Chen certifies that this is the approved version of the following thesis:

C-H Activation by Ozone in Liquid CO_2 Using Cyclohexane and Iso-octane as Substrates

_____

Chair: Bala Subramaniam

Date Approved: _____

Abstract

The study of cyclohexane and isooctane activation by ozone with liquid CO_2 as reaction medium in a Parr reactor equipped with *in situ* infrared detector demonstrated a facile and efficient method for alkane activation. The dominant presence of CO_2 in vapor phase imparts safety to system by maintaining vapor concentration of reactants below the lower flammability limit. At 280 K, 6.9 MPa, with a molar feed ozone: cyclohexane ratio of approximately 50%, the cyclohexane conversion was approximately ~12% with KA oil (a mixture of cyclohexanone and cyclohexanol) yield around 11%. Small but measurable amount of hydrogen peroxide was formed during the reaction. The observed products are consistent with predicted reaction pathways via the hydrotrioxide route. The absence of any detectable water in the product and the close match of cyclohexane conversion and product yield rule out significant combustion of cyclohexane. The various oxygenated products detected from the ozonolysis of isooctane in liquid CO_2 medium suggest that ozone has the ability in activating all types of C-H bonds within isooctane. These results pave the way for systematic investigations of C-H bond activation in lighter alkanes such as methane and those present in natural gas liquids.

Acknowledgments

To my advisor, Dear Prof. Bala Subramaniam, for providing an opportunity to perform research in the challenging area of selective alkane activation using ozone in a novel medium. His patient guidance in research and communication skills were essential for my research to progress smoothly and culminate in this thesis. Most importantly, his requirements for professionalism and perfectness strongly and continually motivate me to improve and become better as a researcher and a professional.

To Prof. Raghunath V. Chaudhari and Prof. Timothy Jackson, for their willingness to serve in my committee, and their precious suggestions on my research.

To Dr. Michael Lundin and Andrew Danby, for their assistance and support in building the experimental apparatus and providing experimental guidance.

To my friends, Kakasaheb Nandiwale, Dupeng Liu, Hongda Zhu, Ziwei Song, Honghong Shi, for their support to my study and life.

To my parents, my sister, for their selfless love and support all the time.

To my source of funding, KBOR (Kansas Board of Regents).

Table of Contents

Abstract iii

Acknowledgments iv

List of Figures viii

Chapter 2 viii

Chapter 3 viii

Appendix viii

List of Tables x

Chapter 1 x

Chapter 2 x

Chapter 3 x

Appendix x

Chapter 1: Introduction and Literature Review 1

1.1 Industrial Application of Ozone 1

1.2 Alkane Activation by Ozone 2

1.3 Utilization of CO_2 5

1.4 Challenge and Opportunity 6

Chapter 2: Ozonolysis of Cyclohexane in Liquid CO_2 8

2.1 Introduction 8

2.2 Phase Behavior Modeling 8

2.3 Lower Flammability Limit for Cyclohexane / O_2 / CO_2 System. 10

2.4 Reactor Unit 11

2.5 Jurgeson® View Cell 15

2.6 Analytical Procedure 15
2.6.1 Product Analysis by GC-MS/FID Method 16
2.6.2 Hydrogen Peroxide Measurement by Ceric Sulfate Titration 17
2.7 Results and Discussion 17
Chapter 3: Ozonolysis of Isooctane in Liquid CO_2 21
3.1 Introduction 21
3.2 Phase Behavior Modeling 21
3.3 Lower Flammability Limit for Isooctane / O_2 / CO_2 System. 23
3.4 Experimental Procedure 24
3.5 Analytical Procedure 24
3.6 Results and Discussion 25
Chapter 4: Conclusions and Recommendations 29
4.1 Conclusions 29
4.2 Recommendations 30
References 32
Appendix 39
1. Cyclohexanol and Cyclohexanone Stayed in Liquid Phase during Reaction. 39
2. Confirmation of Cyclohexanone and Cyclohexanol Formation by GC-MS Method. 39
3. Calibration of Concentrations of Cyclohexane and Products. 39
3.1 Calibration using Organic Solvents by ReactIR. 40
3.2 Calibration of Concentrations of Cyclohexane in Liquid CO_2 by ReactIR. 44
3.3 Calibration by GC-FID. 46
4. Minor Products from Ozonolysis of Cyclohexane. 48

5. Mass Fragmentation Patterns of Products from Ozonolysis of Iso-octane..... 49

List of Figures

Chapter 2

Figure 2-1: Photograph of experimental set-up. 11

Figure 2-2: Photograph of the high-pressure gas reservoir for ozone preparation. 12

Figure 2-3: Photograph of ozone generator used in the experiment. 12

Figure 2-4: Schematic of experimental set-up. 13

Figure 2-5: Photograph of Jurgeson® View Cell for phase separation study. 15

Figure 2-6: GC-FID chromatogram showing cyclohexanone and cyclohexanol products..... 16

Figure 2-7: IR absorbance peaks during ozonolysis of cyclohexane. 18

Figure 2-8: Jurgeson® cell showing two liquid phases for cyclohexanol + CO_2 binary system at 300 K, 6.7 MPa. 18

Chapter 3

Figure 3-1: IR spectra collected during ozonolysis of isooctane. 25

Appendix

Figure A-1: Mass fragmentation pattern of cyclohexanone by GC-MS method. 39

Figure A-2: Mass fragmentation pattern of cyclohexanol by GC-MS method. 39

Figure A-3: IR spectra of cyclohexane, cyclohexanone and cyclohexanol. 40

Figure A-4: IR spectra of cyclohexane and toluene..... 41

Figure A-5: IR spectra of cyclohexanone and hexane. 41

Figure A-6: IR spectra of cyclohexanol and cyclohexane. 42

Figure A-7: Calibration of concentrations of cyclohexane in toluene by ReactIR. 42

Figure A-8: Calibration of concentrations of cyclohexanone in hexane by ReactIR. 43

Figure A-9: Calibration of concentrations of cyclohexanol in cyclohexane by ReactIR. 43

Figure A-10: IR spectra of cyclohexane and liquid CO_2 (280 K, 4.14 MPa). 45

Figure A-11: Calibration of concentrations of cyclohexane in liquid CO_2 (280 K, 4.14 MPa) by ReactIR. 45

Figure A-12: Calibration of concentrations of cyclohexane in acetone by GC-FID. 46

Figure A-13: Calibration of concentrations of cyclohexanone in acetone by GC-FID. 47

Figure A-14: Calibration of concentrations of cyclohexanol in acetone by GC-FID. 47

Figure A-15: Mass fragmentation pattern of 2,2,4-trimethyl-pentanone by GC-MS. 49

Figure A-16: Mass fragmentation pattern of 3,3,5,5-tetramethylbutyrolactone by GC-MS. 49

Figure A-17: Mass fragmentation pattern of acetone by GC-MS..... 49

Figure A-18: Mass fragmentation pattern of 2,4,4-trimethyl-2-pentanol by GC-MS. 50

Figure A-19: Mass fragmentation pattern of 2,2,4-trimethylpentanoic acid by GC-MS..... 50

Figure A-20: Mass fragmentation pattern of tert-butyl alcohol by GC-MS. 50

Figure A-21: Mass fragmentation pattern of pivalic acid by GC-MS. 51

Figure A-22: Mass fragmentation pattern of isobutyric acid by GC-MS. 51

Figure A-23: Mass fragmentation pattern of 2,4,4-trimethyl-1-pentanol by GC-MS. 51

Figure A-24: Mass fragmentation pattern of 2,2,4-trimethyl-1-pentanol by GC-MS. 52

Figure A-25: Mass fragmentation pattern of 2,2,4-trimethyl-3-pentanol by GC-MS. 52

Figure A-26: Mass fragmentation pattern of 2,4-dimethyl-2-pentanol by GC-MS..... 52

Figure A-27: Mass fragmentation pattern of 2,4-dimethyl-2,4-pentanediol by GC-MS. 53

Figure A-28: Mass fragmentation pattern of acetic acid by GC-MS. 53

List of Tables

Chapter 1

Table 1-1: Substrate scope for oxidative C-H functionalization of cycloalkanes. [a] 3

Chapter 2

Table 2-1: Binary interaction parameters for cyclohexane / O_2 / CO_2 system. 10

Table 2-2: Conversion of cyclohexane and yields of products obtained by GC-FID method. [a]. 19

Table 2-3: Measurement of H_2O_2 by ceric sulfate titration. 20

Chapter 3

Table 3-1: Binary interaction parameters for isooctane / O_2 / CO_2 system. 23

Table 3-2: Products and their selectivities from ozonolysis of isooctane. [a] 26

Appendix

Table A-1: Gas phase hydrocarbons detected during ozonolysis of cyclohexane. 39

Table A-2: Distribution of minor products from ozonolysis of cyclohexane. 48

Chapter 1: Introduction and Literature Review

Adipic acid is used in substantial amounts as a precursor for synthesis of Nylon polymer. More than 3.5 million metric tons of adipic acid were produced in 2013,[1] with a projected annual growth rate of 4 - 5%. Although bio-based adipic acid is expected to gain a share of the market the conventional process is expected to dominate the market till at least 2027.[2] In the incumbent industrial process, the synthesis of adipic acid starts with air oxidation of cyclohexane, at temperatures above 398 K and pressures between 0.81 ~ 1.52 MPa, employing Co & Mn catalysts, to produce KA oil (mixture of cyclohexanone and cyclohexanol). The conversion of cyclohexane is usually between 4 ~11% and the selectivity to KA oil is about 85%.[3, 4] The produced KA oil is then oxidized by nitric acid with copper catalysts to synthesize adipic acid with nitrous oxide (N_2O) being emitted as an ozone-depleting greenhouse gas.

1.1 Industrial Application of Ozone

Ozone, as an inorganic molecule with the chemical formula O_3, has a pale blue color in gas phase with a distinctively pungent smell. Ozone has a low solubility in water but is much more soluble in inert non-polar solvents such as CCl_4 or fluorocarbons, in which it forms a blue solution. The ozone in atmosphere is formed from dioxygen by the action of ultraviolet light and electrical discharge. The “ozone layer” that has the highest ozone concentration in the atmosphere protects living beings on earth by absorbing most of the sun’s UV irradiation.

As a strong oxidant, ozone is largely used in the preparation of pharmaceuticals, synthetic lubricants, and many other commercially useful organic compounds, where it is used to sever carbon-carbon double bonds.[5] Ozone has been used in food processing plants where it scrubs yeast and mold spores from the air. Many municipal drinking water systems destroy bacteria with ozone instead of the more common chlorine.[6] Ozone does not form organochlorine compounds,

nor does it remain in the water after treatment. The rapid decay of ozone into dioxygen necessitates its production on site as needed. Once it has decayed, it leaves no taste or odor in drinking water. Many hospitals around the world use large ozone generators, where ozone is generated by electrical discharge, to decontaminate operating rooms between surgeries. The rooms are cleaned and then sealed airtight before being filled with ozone which effectively kills or neutralizes all remaining bacteria.[7]

1.2 Alkane Activation by Ozone

Several studies[8-10] have examined the O_3-facilitated gas phase partial oxidation of methane and ethane at elevated temperatures between 473 - 833 K. Such studies have reported that the rates of methane oxidation correlate strongly with the rates of thermal decomposition of ozone (see Scheme 1). It was reported that the decomposition of ozone into molecular dioxygen and atomic oxygen is a key step in this process.[11]

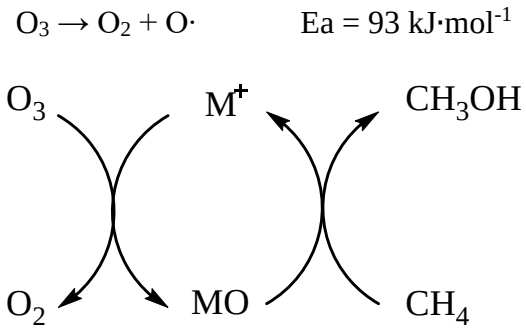

Scheme 1: Catalytic cycle for oxidation of methane with ozone.

Among reported concepts for direct methane conversion, the one involving ozone as an oxidant has been shown to occur at room temperature rather easily with high selectivity for methanol.[12] In this concept, ozone is decomposed at room temperature on a Ni^+ or Pd^+ catalyst to yield a complex with atomic oxygen, which then reacts with methane to produce methanol and

other oxygenated species (see Scheme 1). However, for safety reasons, impractically low methane concentrations were employed in the reported study to avoid flammability.

A relatively recent *Science* publication[13] reported that the ozonolysis of neat cyclohexane to yield adipic acid could be promoted at room temperature by irradiating the reaction mixture with UV irradiation (see Table 1-1).

Table 1-1: Substrate scope for oxidative C-H functionalization of cycloalkanes. [a]

Substrates	Products %Yield	Time (h)	Conversion %	Selectivity for **2** %	%Mass balance
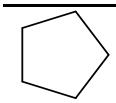 **1a**	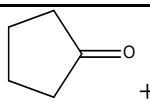 + 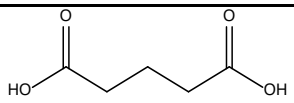 **1a'**8(12) **2a** 50(10)	10	58(22)	86(45)	58(25)
 **1b**	**1d** + 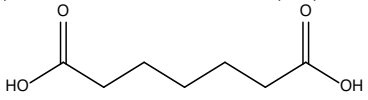 11(15) **2b** 53(13)	15	64(28)	84(46)	54(53)
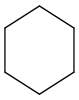 0.5 M HCl	**1d** + 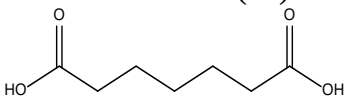 8(10) **2b** 73(45)	15	83(55)	90(82)	83(55)
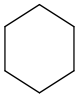	**1b** + **1c** + **1d** + **2b** 68 15 10 trace	0.5	25	---	93
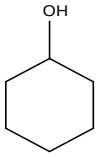 1c	**1c** +**1d**+ 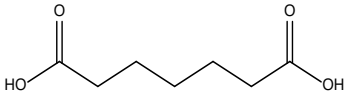 49 40 **2b** 10	0.5	50	20	99
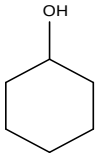	**1d** + 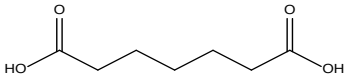 10(15) **2b** 84(25)	8	94(40)	90(63)	98(96)
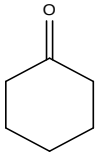 **1d**	**1d** + 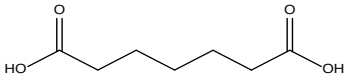 6(65) **2b** 90(30) *	8	90(30)	99(99)	96(95)
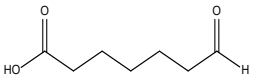 **1e** 2.3M in CCl_4	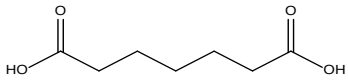 **2b** 99(99)	0.3	99(99)	99(99)	99(99)

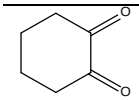 1f 1.0M in CCl_4-1%H_2O		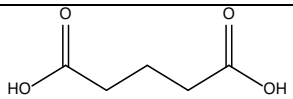 **2a** 97(97)	1.0	97(97)	99(99)	99(99)
 **1g**	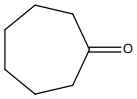 **1g'** 8(12)	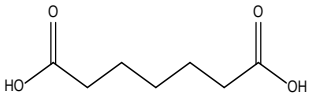 **2g** 65(15)	15	73(27)	90(56)	76(60)
 **1h**	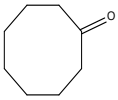 **1h'** 6(12)	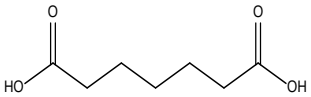 **2h** 70(20)	15	76(32)	92(63)	85(78)

*Addition of 8 vol% aqueous 0.5 M HCl to neat cyclohexanone promotes the adipic acid yield from 30 to 45 mol% at room temperatures in the dark.
[a] Neat liquid substrate was used unless otherwise stated. Reactions were carried out either under UV light, reported first above, or in the dark (reported above in parentheses) at room temperature.

The UV irradiation and aqueous 0.5 M HCl medium are reported to promote the selectivity of adipic acid to 90%. However, it is not clear from the publication if combustion products were formed or not. The UV irradiation aids the decomposition of ozone into $^1O_2$ and atomic oxygen. The mechanism was thought to involve the initial insertion of atomic oxygen into a C-H bond of the cyclohexane rather than its reaction with the singlet oxygen molecule. However, there was still significant reactivity when the reaction was performed in the dark (i.e., without UV radiation). Other authors have claimed an alternative mechanism involving the insertion of the ozone molecule into the C-H bonds of the alkane to form a hydrotrioxide,[14] a species that has been isolated and characterized with several alkanes including iso-pentane, 1,4-dimethylcyclohexane, 1,3-dimethylcyclohexane and decalin.[15] This adduct can then form products in one of the following ways: (a) dissociate to a ketone and hydrogen peroxide; (b) rearrange to form an alcohol and dioxygen molecule; (c) cleave a C-C bond adjacent to the hydrotrioxide to yield an aldehyde and hydroperoxide, which can undergo further oxidation to give carboxylic acid (see Scheme 2). The reaction may have been very sensitive to conditions since another study[16] found no evidence for adipic acid formation, with the ozonolysis of neat cyclohexane producing only cyclohexanone

and cyclohexanol. A review[17] of the mechanistic and kinetic aspects of alkane ozonolysis confirmed the lack of consensus on the mechanism of these reactions.

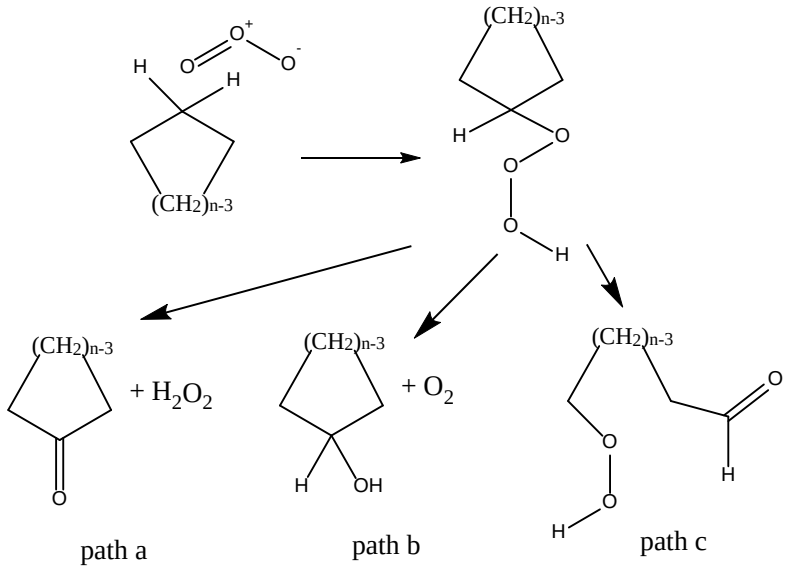

Scheme 2: A possible reaction mechanism for cycloalkane ozonation.

1.3 Utilization of CO_2

Global CO_2 emissions are rising rapidly because of economic growth, boosted largely by the growth of the transportation and manufacturing industries in developing countries in Asia and South America. The global warming caused by steadily increasing atmospheric CO_2 levels has become a worldwide concern in recent years. To combat this increase, methods to capture CO_2 and either store or utilize it are being actively considered. The barriers in this regard include (1) costs of CO_2 capture, separation, purification, and transportation to user site; (2) energy requirements of CO_2 conversion; and (3) the lack of socio-economical driving forces. Yet, in the near term, there may be limited but realistic opportunities to use CO_2 as either feedstock or a tunable and safe solvent medium in chemical reactions and separations.[18] Examples include the use of CO_2 in the synthesis of organic chemicals [19-24], chemical conversion of CO_2 [25-30], syngas

production by dry reforming with CH_4 [30-34], use of supercritical CO_2 as a reactant or medium [35-38], polymer synthesis and processing using supercritical CO_2 [39, 40].

Supercritical CO_2 (SC-CO_2) has been used for extraction of various substances ranging from beverage materials (such as caffeine from coffee bean), foods, organic and inorganic functional materials, to herbs and pharmaceuticals. Meanwhile, supercritical CO_2 can be used as a solvent or reaction medium for a number of organic reactions, for homogenous catalysis involving hydrogenation, transition metal catalysis, palladium-mediated couplings, radical reactions and polymerizations [41]. The Subramaniam group has studied oxidations in CO_2-based reaction media, including novel CO_2-expanded phases.[42, 43] CO_2-expanded liquid (CXL) or liquid CO_2 media offer several advantages as follows: either partial or total replacement of conventional organic solvents with dense CO_2 at moderate pressures (tens of bars), enhanced O_2 solubility in the CXL media which is pressure-tunable; and to shrink or eliminate vapor phase flammability as CO_2 is a flame retardant. Herein, we investigate the use of liquid CO_2 as a safe reaction medium for ozonolysis.

1.4 Challenge and Opportunity

Despite its immense potential for direct and selective oxidation of alkanes, the use of ozone will remain an academic curiosity unless safe methods that eliminate vapor phase flammability are demonstrated. To overcome this gap, the Subramaniam group has been investigating the use of liquid carbon dioxide as a safe reaction medium for performing alkane partial oxidation facilitated by ozone. This thesis details the first attempts in this area using cyclohexane and isooctane as substrates.

CO_2 is inert to ozone and non-toxic. Further, CO_2 is abundant and inexpensive. The Subramaniam group has recently reported that liquid CO_2 dissolves ozone in high concentration

and that the ozonolysis of methyl oleate can be performed at high rate and selectivity in liquid CO_2.[44, 45] For systems containing liquid CO_2, the vapor phase consisting of dense CO_2 will impart safety to the reaction by avoiding flammability.[46] The objectives of this thesis are to investigate the feasibility of performing ozonolysis in liquid CO_2 using cyclohexane and isooctane as model substrates and without using an ozone decomposition catalyst. Toward this end, a stirred batch reactor equipped with *in situ* ReactIR monitoring capability was constructed to investigate the conversion of these substrates to various products. We decided to establish the process concept with alkanes that are liquids at ambient conditions and hence do not present safety issues with respect to vapor phase flammability. The results from this research are expected to provide guidance and justification for future work involving lighter alkanes.

Chapter 2: Ozonolysis of Cyclohexane in Liquid CO_2

2.1 Introduction

To establish safe operating conditions, knowledge of vapor liquid equilibrium of the reaction mixture is essential. Further, a reactor setup capable of performing ozonolysis of alkanes in a safe manner is essential. Finally, reliable analysis of the products is essential to interpret the reaction pathways and establish feasibility of the proposed concept. This chapter addresses both experimental and modeling research that were undertaken to address these aspects.

2.2 Phase Behavior Modeling

Vapor-liquid equilibrium (VLE) modeling for cyclohexane / oxygen / carbon dioxide mixture was performed by using Aspen Plus V9. Even though ozone is involved in the actual reaction mixture, its concentration is relatively small (~ 4 mol% O_3 in O_2/O_3 mixture). Thus, the molar concentration of O_3 in the initial reaction mixture is approximately 1 %. Hence, the vapor phase composition using the cyclohexane/O_2/CO_2 ternary at reaction conditions was considered sufficient to assess vapor phase flammability. A flash separator at 6.9 MPa and 280 K was considered for phase behavior calculation, with the ternary feed mixture separating into liquid and vapor phases at equilibrium. The molar feed mixture was taken to be 2.3 % cyclohexane, 70 % CO_2 and 27.7 % O_2, with the O_2 mole fraction representing the overall O_2+O_3 mole fraction in the actual feed used in the ozonolysis experiments. Binary interaction parameters k_{ij} were calculated through regression by Aspen Plus using Peng- Robinson EOS and VLE experimental data from the literature.[47-49] The calculated binary interaction parameters are listed in Table 2-1.

Peng- Robinson EOS:

$$P = \frac{RT}{V-b_i} - \frac{a_i(T)}{V(V+b_i)+b_i(V-b_i)}$$

R= 8.314 mL· MPa · mol^{-1}· K^{-1}

$$b_i = 0.0777960739 \frac{RT_{c,i}}{P_{c,i}}$$

$$a_i = 0.457235529 \frac{R^2 {T_{c,i}}^2}{P_{c,i}} \left[1 + m_i \left(1 - \sqrt{\frac{T}{T_{c,i}}}\right)\right]^2$$

if $\omega_i \leq 0.491$, $m = 0.37464 + 1.54226\omega_i - 0.26992\ {\omega_i}^2$

if $\omega_i > 0.491$, $m = 0.379642 + 1.48503\omega_i - 0.164423{\omega_i}^2 + 0.016666{\omega_i}^3$

Classical mixing rule

$$a = \sum_{i=1}^{N} \sum_{j=1}^{N} z_i z_j \sqrt{a_i a_j}(1 - kij\ (T))$$

$$b = \sum_{i=1}^{N} z_i b_i$$

Where,

P = Pressure (MPa)

V = Molar volume (the volume of 1 mole of gas or liquid, mL · mol^{-1})

T = Temperature (K)

R = Ideal gas constant (8.314 mL · MPa · mol^{-1}· K^{-1})

T_c = Critical temperature (K)

P_c = Critical pressure (MPa)

a, b = Substance-specific constants calculated from critical properties as shown above (a with unit mL^2 · MPa · mol^{-2}, b with unit mL · mol^{-1})

ω = acentric factor of species (unitless)

m = Pure component factor (unitless)

z = Compressibility factor (unitless) = $\frac{PV}{RT}$ (V= molar volume, mL · mol^{-1})

kij = Binary interaction parameter between species i and j (unitless)

Table 2-1: Binary interaction parameters for cyclohexane / O_2 / CO_2 system.

Components	k_{ij}
CO_2 - cyclohexane	0.1659
CO_2 - O_2	0.1556
O_2 - cyclohexane	0.2078

The molar vapor phase composition is estimated to be 0.6 % cyclohexane, 30.5% O_2 and 68.9% CO_2.

2.3 Lower Flammability Limit for Cyclohexane / O_2 / CO_2 System.

The lower flammability limit (LFL) for cyclohexane - air mixture is reported to be 1.3 mol% at 298 K, 0.1 MPa. [50] The LFL doesn't change when replacing air with oxygen, [51] but is likely to increase when the temperature decreases from 298 to 280 K according to the following equation (Eq. 1) that correlates the LFL dependence on temperature. [46]

$$LFL_T = LFL_{25} - \frac{0.75}{\Delta H_C}(T\text{-}25) \quad (1)$$

where,

T = Temperature (℃)

LFL_T = Lower flammability limit at temperature T (℃)

LFL_{25} = Lower flammability limit at 25 ℃

ΔH_C = Heat of combustion (kJ· mol^{-1})

According to Eq. 1, the LFL of cyclohexane / O_2 / CO_2 system is estimated to be 1.31 mol%, at 280 K and 6.9 MPa, since pressure is known to have only a minor effect on the LFL. [51] Based on the phase equilibrium calculation, the vapor phase concentration of cyclohexane (~0.6 mol%), corresponding to the cyclohexane/O_2/CO_2 ternary at initial reaction conditions, is well

below the estimated LFL. This conclusion is justified considering (a) the significant presence of CO_2 (a flame retardant) in the vapor phase, and (b) that the major products such as cyclohexanone and cyclohexanol are less volatile than cyclohexane and hence will be primarily in the liquid phase at reaction conditions. This was confirmed by an analysis of the vented gas mixture that showed much lower amounts of cyclohexanol and cyclohexanone compared to cyclohexane (see Table A-1 in Appendix, Section 1).

2.4 Reactor Unit

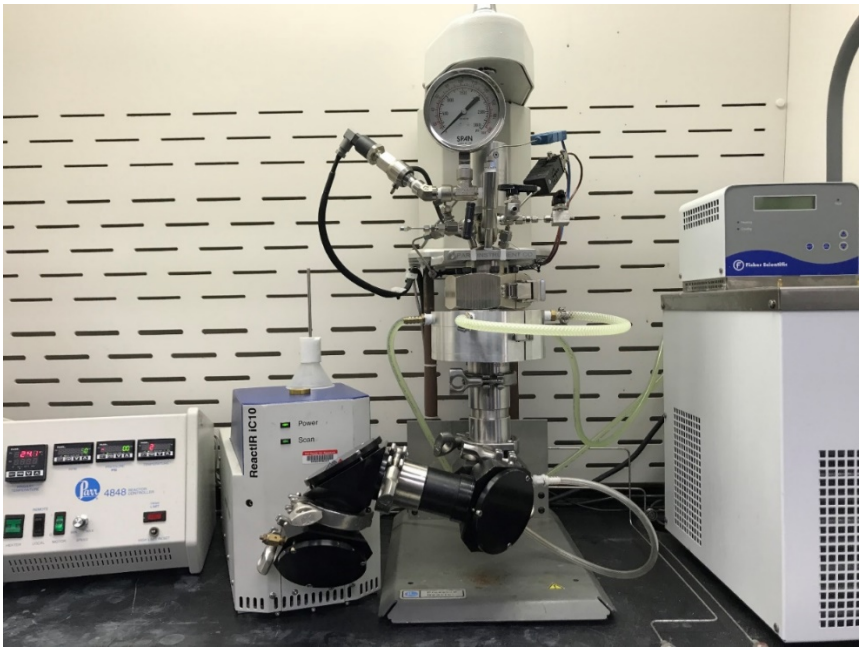

Figure 2-1: Photograph of experimental set-up.

Figure 2-2: Photograph of the high-pressure gas reservoir for ozone preparation.

Figure 2-3: Photograph of ozone generator used in the experiment.

A schematic of the experimental unit is given in Figure 2-4. Photographs of the various experimental units used in this thesis research are shown in Figures 2-1 – 2-3. The ozone-facilitated C-H activation in liquid CO_2 was investigated using a Parr reactor, with the reaction progress followed by an *in situ* ReactIR probe. Ozone was produced on site from oxygen by a Praxair Unizone ozone generator, producing a stream with an ozone concentration of approximately 4 (v/v) %. All chemicals were used as purchased without further purification. Cyclohexane (99.9%), Acetone (99.9%), were purchased from Sigma-Aldrich. Oxygen (extra dry) and Carbon dioxide were ordered from Matheson.

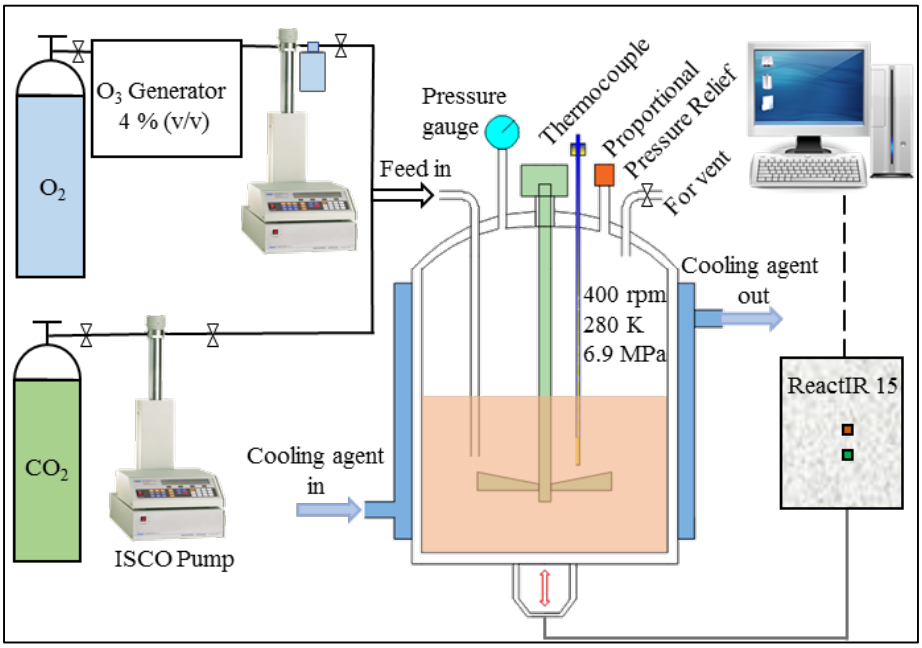

Figure 2-4: Schematic of experimental set-up.

In a typical reaction, the following protocol was followed with the set-up in Figure 2-4:

1) Liquid nitrogen was added to the ReactIR 15 instrument and the IR probe was configured after cooling for 30 minutes;
2) 1 mL of cyclohexane was added to the 50 mL Parr reactor which was then sealed.

3) The reactor was cooled down to 280 K and then CO_2 was added to the reactor by an ISCO pump to achieve a total liquid volume of 15 mL and the liquid mixture was stirred at 400 rpm.
4) A 250 mL gas cylinder was filled with the ozone/oxygen mixture (293 K, 507 mL, 0.59 MPa) using the Praxair Unizone ozone generator. Multiple volumes of the ISCO pump were used to fill this gas cylinder, which was used as a high-pressure reservoir for the ozone/oxygen gas. This filling method was confirmed to have no influence on ozone quality by other researchers in our group[44];
5) Using the ozone/oxygen gas from the reservoir to fill the ISCO pump following the final stroke, the ozone/oxygen gas was pumped through a unidirectional valve into the reactor to a pressure of 6.9 MPa. This was considered as t_0 for the reaction. Ozone was added after the cyclohexane/ CO_2 binary had reached equilibrium with pressure and temperature stabilized, and the stir was kept running during and after adding ozone.
6) After one hour following reactor pressurization with the O_3/O_2 mixture (with reaction solution continually monitored by the ReactIR probe), the stirrer was stopped, and the reactor was cooled as rapidly as possible to 274 K.
7) The reactor was depressurized to atmospheric pressure by venting the CO_2 at 274 K. The gas phase exiting the reactor during depressurization was bubbled slowly through a 300 mL acetone trap at 273 K (in an ice bath). The acetone trap was designed to capture any volatile products discarded by depressurization. The acetone mixture was then analyzed by GC -MS and FID methods.
8) Following this step, 35 mL of acetone were added to the reactor following by stirring at 350 rpm to dissolve the products in acetone.
9) The diluted samples in acetone were prepared for GC-MS and GC-FID analyses.

The carbon balance (on a CO_2-free basis) was improved significantly when the reactor was depressurized at 273 K (following step#7) compared to reactor depressurization at ambient temperature.

2.5 Jurgeson® View Cell

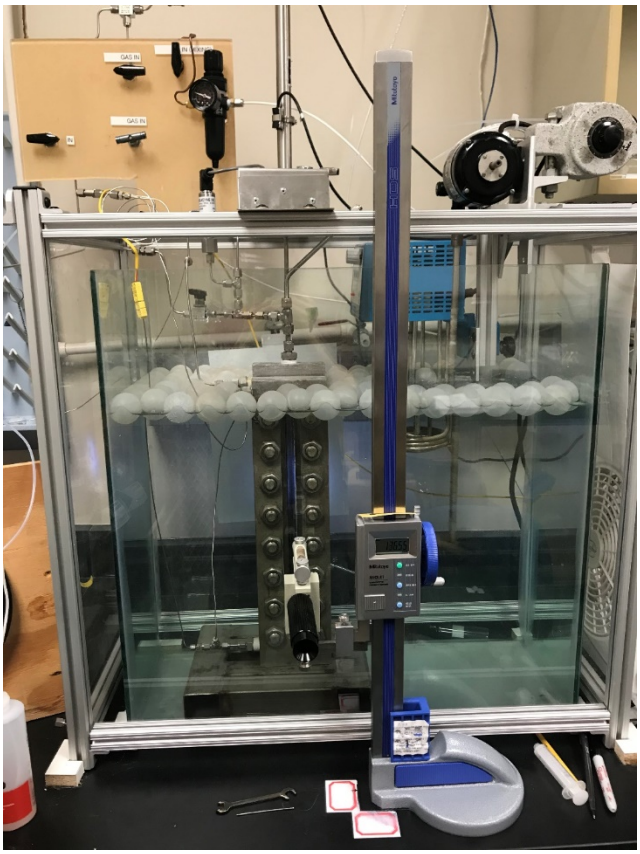

Figure 2-5: Photograph of Jurgeson® View Cell for phase separation study.

During a phase equilibrium study in a Jurgeson® view cell (Figure 2-5), 4 mL cyclohexanol was added to the view cell that was maintained at 300 K in a water bath. Then liquid CO_2 was pumped into the view cell to a total volume of 48 mL (300 K, 6.7 MPa). The two liquid layers were agitated vigorously to accelerate the mixing process, and then allowed to separate to check for immiscibility. A similar protocol was followed for studying the miscibility between cyclohexane and cyclohexanone with liquid CO_2, respectively.

2.6 Analytical Procedure

2.6.1 Product Analysis by GC-MS/FID Method

The GC (Gas Chromatography) method uses an HP-INNOWAX column on an Agilent 7890A GC coupled to a 5975C MS (Mass Spectrometry) and uses a carrier He gas flow of 1 std·cm^3 ·min^{-1}, an inlet temperature of 523 K, and an injection volume of 1 µL. The oven temperature was initially held at 313 K for 5 minutes, then ramped at 10 K per minute to 493 K and held at this temperature for a further 20 minutes. Neat cyclohexane was analyzed by GC-FID method to identify impurities. Cyclohexanone and cyclohexanol in acetone solution were tested to determine retention times of both compounds in GC-FID chromatogram. Preliminary experiments indicated that two peaks with the largest areas from GC-FID chromatogram had the same retention time as cyclohexanone and cyclohexanol (see Figure 2-6).

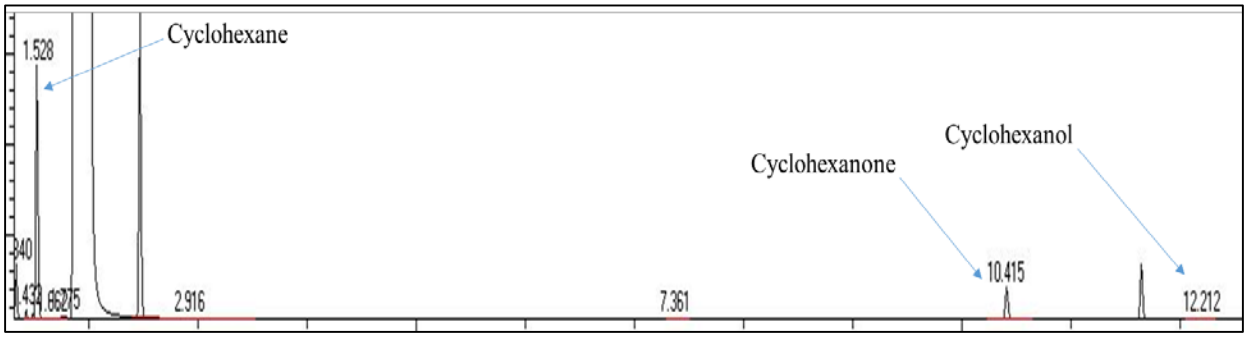

Figure 2-6: GC-FID chromatogram showing cyclohexanone and cyclohexanol products.

GC-MS method also confirmed the formation of cyclohexanone and cyclohexanol (see Figure A-1 and Figure A-2 in Appendix, Section 2). Minor products were to be identified by analyzing GC-MS chromatogram. Calibrations of product concentrations for quantification purpose were focused on these two compounds. The detection of water (as evidence of combustion product) was attempted by GC-MS method.

2.6.2 Hydrogen Peroxide Measurement by Ceric Sulfate Titration

Ceric sulfate solution was used to detect the formation of any hydrogen peroxide during reaction. The reaction mechanism for titration is described in Eq.2. A few drops of ferroin indicator solution with pink color was added to 150 mL sulfuric acid (5 (v/v) %, $<$ 280 K), then the solution was titrated by ceric sulfate solution (0.1N) to a bright green color. A certain amount of product solution was added to this bright green solution, which then changed back to pink color. This pink colored solution was titrated by ceric sulfate solution back to bright green color as ending point. The mass of these chemicals consumed during the titration process was used to quantify hydrogen peroxide according to Eq. 3.

$$H_2O_2 + 2\ Ce(SO_4)_2 = Ce_2(SO_4)_3 + H_2SO_4 + O_2 \qquad (2)$$

$$H_2O_2\ w\% = \frac{\text{Volume of ceric sulfate (L)} \times 0.1\ \text{mol}\cdot\text{L}^{-1} \times 0.5 \times 34.01\ \text{g}\cdot\text{mol}^{-1}}{\text{Weight of sample (g)}} \times 100\% \qquad (3)$$

2.7 Results and Discussion

The temporal IR spectra of cyclohexane consumption and product (cyclohexanol and cyclohexanone) evolution during ozonolysis were recorded by ReactIR as shown in Figure 2-7. The peak growth with time at 1712 cm^{-1} indicates that the products (cyclohexanone and cyclohexanol) were formed during the reaction. Quantification based on IR spectra is complicated by the fact that cyclohexanol is not miscible in the reaction mixture. A study of cyclohexanol miscibility in liquid CO_2 in a Jurgeson® cell confirmed that while cyclohexane and cyclohexanone are miscible with liquid CO_2 at ambient temperature, cyclohexanol is not (see Figure 2-8). The figure clearly shows two liquid phases with cyclohexanol condensed at the bottom of a liquid CO_2 layer. This phase separation will lead to the observed saturated absorbance at 1712 cm^{-1} and could also have contributed to the drift of the spectra as shown in Figure 2-7.

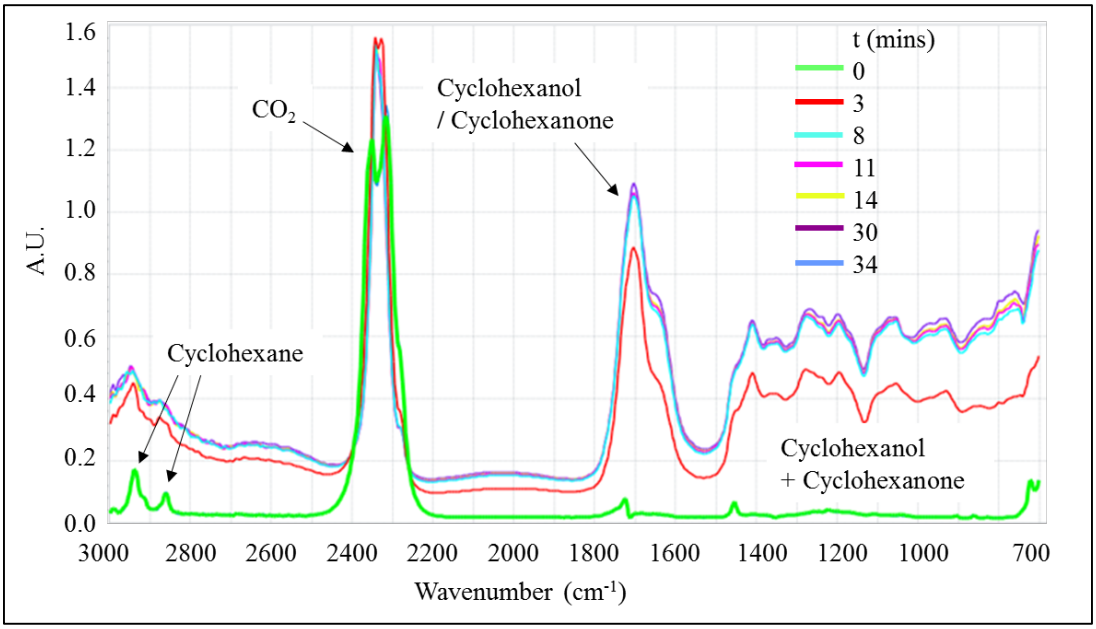

Figure 2-7: IR absorbance peaks during ozonolysis of cyclohexane. (operating conditions are given in Table 2-2)

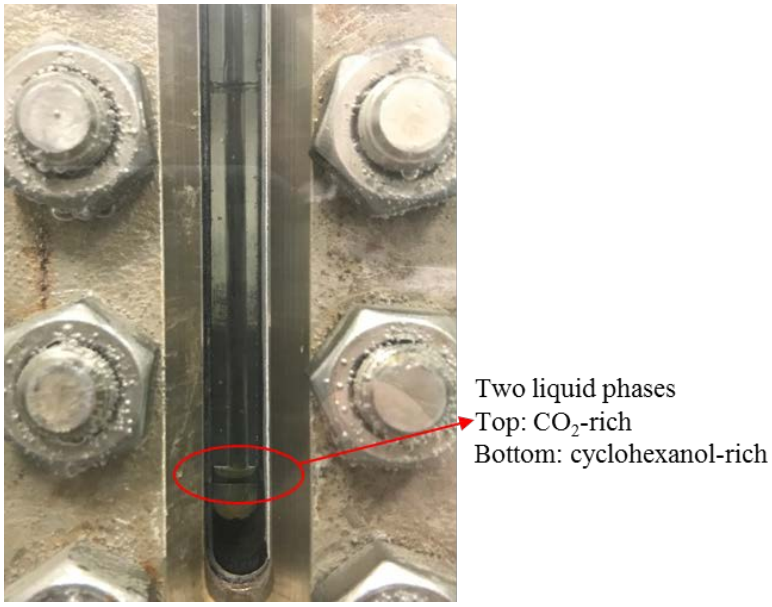

Figure 2-8: Jurgeson® cell showing two liquid phases for cyclohexanol + CO_2 binary system at 300 K, 6.7 MPa.

For reliable quantification of the reactant and products, GC-FID analysis was performed on the contents remaining in the reactor at the end of the run and the hydrocarbon species collected externally from the gas phase (see Table 2-2).

Table 2-2: Conversion of cyclohexane and yields of products obtained by GC-FID method. [a]

Entry	O_3: Cyclohexane (mol%)	Carbon Closure (%)	Conversion of Cyclohexane (%)	KA Oil Yield[b] (mol%)	Cyclohexanone : Cyclohexanol	H_2O_2 (mol) × 10^{-5}
1	49	88	11.6	10.8	102	8.6
2	51	94	12.4	11.5	125	9.6
3	55	91	12.9	11.9	111	9.2
4	150	94	19.4	18.5	109	35

[a]Reaction conditions: 9.22×10^{-3} mol cyclohexane, 280 K, 6.9 ± 0.3 MPa, 400 rpm, 1 hr.
[b] Conversion of Cyclohexane = (Moles of cyclohexane reacted)/ initial moles of cyclohexane. KA Oil Yield = (Moles of cyclohexanone and cyclohexanol produced)/ initial moles of cyclohexane.

The results show that with an ozone: cyclohexane molar ratio of approximately 50%, the cyclohexane conversion was ~12%, with KA oil (mixture of cyclohexanone and cyclohexanol) yield being approximately 11%. The relatively minor differences between the conversion and yield values in Table 2-2 is consistent with the C balance (considering only organic carbon) and reflect the insignificant production of minor products. Tripling the ozone: cyclohexane molar feed ratio increases cyclohexane conversion and KA oil yield by roughly 150%. In sharp contrast, the H_2O_2 formation (see Scheme 2), increases several folds albeit still low compared to the other products. Hydrogen peroxide was measured using ceric sulfate titration as shown in Table 2-3. Several minor products including 1,4-cyclohexanedione, hydroxy cyclohexanone and a few derived from ring opening (butyrolactone, oxalic acid, etc.), were detected at low concentrations, having a combined yield of approximately 0.80 mol% (see Table A-2 in Appendix, Section 4).

Table 2-3: Measurement of H_2O_2 by ceric sulfate titration.

Entry	Sample amount (g)	Sulfuric acid (mL)	Ceric sulfate solution (g)	Mass percentage (%)	Mass in 35 mL product solution (g)	Mol. of H_2O_2 in 35 mL product solution
1	5.2896	150	0.3423	0.0138	3.3×10^{-3}	9.6×10^{-5}
2	5.2284	150	0.3267	0.0133	3.2×10^{-3}	9.3×10^{-5}

*Reaction condition: 9.22×10^{-3} mol cyclohexane, O_3/cyclohexane = 51%. 280 K, 6.9 MPa, 400 rpm, 1 hr. The titration was repeated twice for each product sample, as entry 1 and entry 2.

Although a trace of water was detected in the products using GC-MS method, it is most likely an impurity in acetone. The near-absence of water in the product mixture suggests insignificant combustion of cyclohexane. This is also consistent with the high CO_2-free carbon balance (~90%) between the reactant and detected hydrocarbon products.

It is clear from the foregoing results that cyclohexane undergoes facile ozonolysis in liquid CO_2 to yield cyclohexanone as the major products. This result is consistent with the previous study by Barletta [16] that showed production of cyclodecanone from ozonolysis of cyclodecane, and no adipic acid formation from ozonolysis of cyclohexane. However, in contrast to the reported results of Hwang,[13] where the reaction times were ~15 h, no adipic acid was detected in this study. The fact the ozone is reported to selectively activate only the terminal bonds and not the internal bonds is in sharp contrast to our observation wherein ozone activates all C-H bonds in *iso*octane (see Chapter 3). Further, the yield of KA oil via the ozonolysis process (11%) is achieved in ~ 10 mins (see Figure 2-7) and the yield is greater than the conventional process (8.5%) where high temperatures (423 ~433 K) and pressure (0.81 ~ 1.52 MPa) are necessary for catalytic oxidation of cyclohexane by Co and Mn catalysts in air. [3,4] The residence time required in conventional process is typically on the order of several tens of minutes.

Chapter 3: Ozonolysis of Isooctane in Liquid CO_2

3.1 Introduction

Chapter 2 demonstrated proof-of-concept for C-H bond activation in liquid CO_2 by using cyclohexane as the model substrate. The equipment and analytical methods provide a strong foundation for extending the study to activate C-H bonds in linear alkanes. While the ultimate goal of the program is to activate such bonds in light alkanes including methane using ozonolysis, the approach of the Subramaniam group is to first test the concept with linear alkanes that are liquids at ambient conditions, such as isooctane. The reasons are as follows: (1) The linear alkanes are miscible in liquid CO_2, and (2) The vapor phase concentrations in the presence of liquid CO_2 are small enough to maintain them below the lower flammability limit even in the presence of oxygen/ozone mixture. This chapter provides results of preliminary investigations of isooctane ozonolysis in liquid CO_2.

3.2 Phase Behavior Modeling

Vapor-liquid equilibrium modeling for isooctane / oxygen / carbon dioxide mixture was performed by Aspen Plus V9. The procedure is similar to that used for modeling the cyclohexane/O_2/CO_2 ternary system (see Chapter 2, Section 2). Binary interaction parameter k_{ij} for O_2 / CO_2 binary system was calculated through regression of experimental data from literature[48] by using Aspen Plus with Peng- Robinson EOS. The k_{ij} value for O_2 / isooctane binary system was calculated by Eq.4, [52] with T_c (critical temperature of pure component). $T_{c,1}$ = 154.6 K (O_2), $T_{c,2}$ = 543.9 K (isooctane).

$$k_{1,2} = 1 - 2\,(T_{c,1} * T_{c,2})^{1/2} / (T_{c,1} + T_{c,2}) \qquad (4)$$

*k*ij for CO_2 / isooctane binary mixture was calculated by equation developed based on PR78 EOS in the literature[53].

Equations developed based on PR78 EOS:

$$P = \frac{RT}{V - b_i} - \frac{a_i(T)}{V(V + b_i) + b_i(V - b_i)}$$

$$b_i = 0.0777960739 \frac{RT_{c,i}}{P_{c,i}}$$

$$a_i = 0.457235529 \frac{R^2 {T_{c,i}}^2}{P_{c,i}} \left[1 + m_i \left(1 - \sqrt{\frac{T}{T_{c,i}}}\right)\right]^2$$

if $\omega_i \leq 0.491$, $m = 0.37464 + 1.54226\omega_i - 0.26992\ {\omega_i}^2$

if $\omega_i > 0.491$, $m = 0.379642 + 1.48503\omega_i - 0.164423{\omega_i}^2 + 0.016666{\omega_i}^3$

$$k_{12}(T) = \frac{A_{12}\left(\frac{298.15}{T}\right)^{\left(\frac{B_{12}}{A_{12}} - 1\right)} - \left(\frac{\sqrt{a_1(T)}}{b_1} - \frac{\sqrt{a_2(T)}}{b_2}\right)^2}{2\frac{\sqrt{a_1(T)a_2(T)}}{b_1 b_2}}$$

$\omega_{CO_2} = 0.225, \omega_{isooctane} = 0.304$

A_{12} = 129.95 MPa, B_{12} = 298.82 MPa

where,

P = Pressure (MPa)

V = Molar volume (the volume of 1 mole of gas or liquid, mL· mol^{-1})

T = Temperature (K)

R = Ideal gas constant (8.314 MPa · mL · mol^{-1}· K^{-1})

T_c = Critical temperature (K)

P_c = Critical pressure (MPa)

a, b = Substance-specific constants calculated from critical properties as shown above (a with unit mL^2 · MPa · mol^{-2}, b with unit mL · mol^{-1})

ω = acentric factor of species (unitless)

m = Pure component factor calculated from ω (unitless)

k_{12} = Binary interaction parameter between CO_2 and isooctane (unitless)

A_{12}, B_{12} = Parameters defined in the literature[53] (MPa)

The calculated binary interaction parameters are listed in Table 3-1.

Table 3-1: Binary interaction parameters for isooctane / O_2 / CO_2 system.

Components	kij
O_2-Isooctane	0.1697
CO_2-Isooctane	0.1068
O_2-CO_2	0.1556

The vapor phase concentration of isooctane was calculated to be ~ 0.3 mol% corresponding to the initial composition of isooctane, CO_2 and O_2 at reaction conditions [280 K, 6.2 MPa, molar ratio for isooctane/CO_2/O_2 = 3/69/28]. Since the ozone concentration in oxygen is low (~4 mole%), its concentration in the initial feed mixture will be still low (~ 1 mole%). Hence, the ozone content in the feed was ignored to model the system as a pseudo-ternary system.

3.3 Lower Flammability Limit for Isooctane / O_2 / CO_2 System.

The lower flammability limit (LFL) for isooctane - air mixture is 0.95 mol% at 298 K, 0.1 MPa.[46] The LFL doesn't change when replacing air with oxygen, [51] but is likely to increase when the temperature decreases from 298 to 280 K according to the temperature dependence of LFL (see Eq. 1). [46]

$$LFL_T = LFL_{25} - \frac{0.75}{\Delta H_C}(T\text{-}25) \quad (1)$$

where,

T = Temperature (℃)

LFL_T = Lower flammability limit at temperature T (℃)

LFL_{25} = Lower flammability limit at 25 ℃

ΔH_C = Heat of combustion (kJ· mol^{-1})

According to Eq. 1, the LFL of isooctane / O_2 / CO_2 system is estimated to be 0.95 mol% at 280 K and 6.2 MPa, since pressure is known to have only a minor effect on the LFL. [51] Based on the phase equilibrium calculation, the vapor concentration of isooctane (~0.3 mol%), corresponding to the isooctane/O_2/CO_2 ternary at initial reaction conditions, is well below the estimated LFL. This conclusion is justified considering (a) the significant presence of CO_2 (a flame retardant) in the vapor phase, and (b) that the major products such as 2,2,4-trimethyl-pentanone and 3,3,5,5-tetramethylbutyrolactone are less volatile than isooctane and hence will be primarily in the liquid phase at reaction conditions.

3.4 Experimental Procedure

The experimental procedure is similar to that used for studying cyclohexane ozonolysis except that THF instead of acetone was used as a solvent to recover the products from the reactor at the end of the reaction. The gas phase hydrocarbons were not collected during depressurization at this preliminary investigation.

3.5 Analytical Procedure

Products from ozonolysis of isooctane were collected first by adding cyclohexane to the reactor after venting CO_2. The sample was then diluted in cyclohexane and analyzed by GC-MS and FID methods. To avoid peak overlapping in the chromatogram between cyclohexane and possible products, another experiment at same reaction condition was repeated with THF as solvent for product collection after reaction. Neat cyclohexane, hexane, THF, isooctane and standard solutions of isooctane in cyclohexane, acetone in cyclohexane, tert-butyl alcohol in cyclohexane, acetone in THF were prepared and analyzed by GC-MS and GC-FID methods. The chromatograms generated from above solutions were used to identify impurities from solvents and

products from the reaction by comparison. THF was chosen as solvent for product collection as cyclohexane co-elutes with isooctane and hexane contains isooctane as an impurity.

Ceric sulfate solution was used to detect and quantify the formation of hydrogen peroxide during reaction. GC-MS method was used to detect any water formation as a product of combustion.

3.6 Results and Discussion

The temporal IR spectra of reactant consumption and product evolution are shown in Figure 3-1. IR absorbance peaks for CO_2 and isooctane are labeled as shown in Figure 3-1**.** IR peaks for products are to be identified in future studies. The decrease in the isooctane peaks with time and the simultaneous appearance of various growing peaks in the IR spectra provide evidence of isooctane consumption toward possible products. The product mixture was collected and analyzed at the end of the run to identify the products formed.

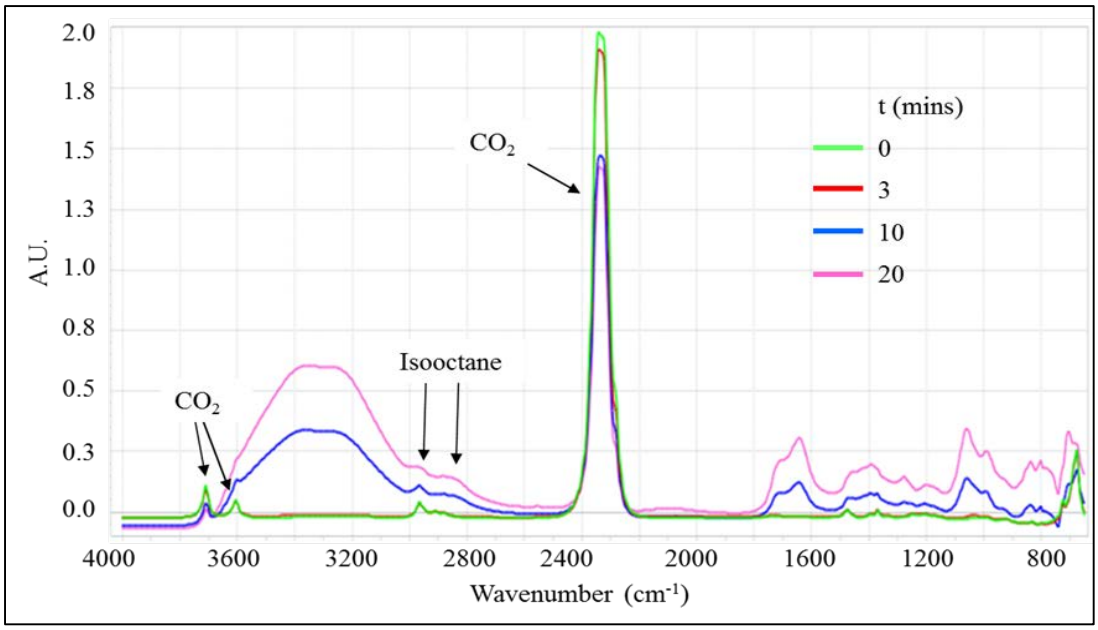

Figure 3-1: IR spectra collected during ozonolysis of isooctane.

(given reaction condition in Table 3-2)

Based on the GC-MS chromatogram of products, the identified products are listed in Table 3-2. The GC-MS fragmentation patterns of the various products are given in Appendix (Figure A-15 – A-28). No water could be detected by the GC-MS which indicates combustion reaction is not favored at these conditions. It is worth noting that 4.6×10^{-5} mol H_2O_2 was detected by ceric sulfate titration method from the reaction.

Table 3-2: Products identified by GC-MS from ozonolysis of isooctane. [a]

Entry	Name	Formula	Structure
1	2,2,4-Trimethyl-pentanone	$C_8H_{16}O$	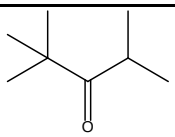
2	3,3,5,5-Tetramethylbutyrolactone	$C_8H_{14}O_2$	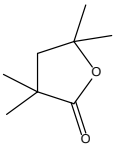
3	Acetone	C_3H_6O	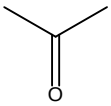
4	2,4,4-Trimethyl-2-pentanol	$C_8H_{18}O$	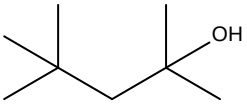
5	2,2,4-Trimethylpentanoic acid	$C_8H_{16}O_2$	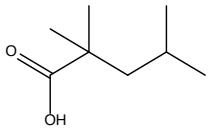
6	Tert-butyl alcohol	$C_4H_{10}O$	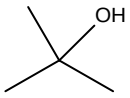
7	Pivalic acid	$C_5H_{10}O_2$	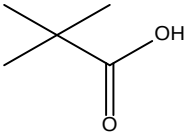
8	Isobutyric acid	$C_4H_8O_2$	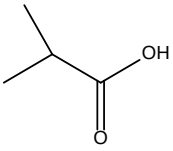

9	2,4,4-Trimethyl-1-pentanol	$C_8H_{18}O$	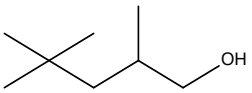
10	2,2,4-Trimethyl-1-pentanol	$C_8H_{18}O$	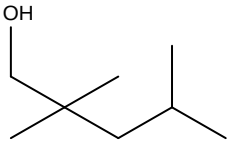
11	2,2,4-Trimethyl-3-pentanol	$C_8H_{18}O$	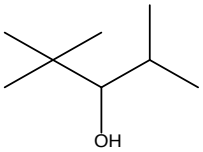
12	2,4-Dimethyl-2-pentanol	$C_7H_{16}O$	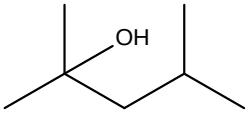
13	2,4-Dimethyl-2,4-pentanediol	$C_7H_{16}O_2$	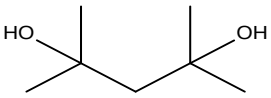
14	4,4-Dimethyl-2-pentanol	$C_7H_{16}O$	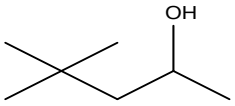
15	Acetic acid	$C_2H_4O_2$	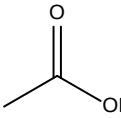
16	Unknown acid	-	-

[a] Reaction conditions: 280 K, 6.2 MPa, 400 rpm, 1 hr. 2 mL isooctane, ozone: isooctane = 38 mol%.

The strong IR absorbance between 800 ~ 1800 cm^{-1} in the IR spectra (Figure 3-1) seems to indicate phase separation of products from liquid CO_2. The IR absorbance peak at 3400 cm^{-1} could either result from water condensing on IR probe lens or hydrogen peroxide formation. Karl Fischer titration will provide an alternative way other than GC-MS method to detect water, but avoiding water vapor from air during analysis is a challenge.

The ozonolysis of isooctane produced various kinds of oxygenated products including alcohol, ketone and acids. Chain-scission products, such as C_2-C_7, were also detected while the

possible formation of C_9 or higher species is yet to be determined. The activation of both terminal and internal C-H bonds in *iso*octane by ozone is in sharp contrast to the highly selective activation of the terminal bonds during cyclohexane ozonolysis to directly produce adipic acid (90% selectivity). [13]

Chapter 4: Conclusions and Recommendations

4.1 Conclusions

A process concept for ozonolysis of cyclohexane and isooctane in liquid CO_2 at near-ambient conditions was successfully demonstrated. The ozonolysis proceeds at reasonable reaction rates with high selectivity towards oxygenated products and no detectable formation of combustion products resulting in high C (~90%) atom economy.

The primary products formed during cyclohexane ozonolysis are cyclohexanone (K) and cyclohexanol (A) with the K/A ratio being ~120 in most cases. Traces of hydrogen peroxide were also detected. These products are consistent with predicted reaction pathways. Significantly, the yield of the desired cyclohexanone product is significantly higher at much shorter reaction times compared to the conventional process for cyclohexane oxidation. Further, the current process is environmentally friendlier as it does not use nitric acid as an oxidant, which results in N_2O emissions. Although toxic, the ozone is contained in the reactor and used completely for reaction. Any low-level ozone emissions eventually decompose to oxygen.

Temporal reactant consumption and product evolution profiles were monitored by performing the reaction in a Parr reactor equipped with a ReactIR probe. Quantification of cyclohexane, cyclohexanol and cyclohexanone as well as identification of minor products were performed by GC/FID analysis. Safe operating conditions were determined based on vapor/liquid phase equilibrium predictions of the ternary cyclohexane/O_2/CO_2 system based on data from literature sources. Such predictions help ensure that the reactor operating conditions are chosen to achieve vapor phase composition that is below the lower flammability limit.

Isooctane ozonolysis also selectively produces oxygenated products with no detectable formation of water. Even though the isooctane conversion and products have only been quantified

using approximate GC/FID methods, the various identified products have demonstrated the ability of ozone in oxidizing all types of C-H bonds in alkane. As for cyclohexane ozonolysis, it was possible to follow isooctane consumption and product formation by ReactIR probe. Further, safe operating conditions were determined based on prediction of vapor liquid phase behavior to confirm that the vapor phase concentration of isooctane at operating conditions was below the lower flammability limit.

4.2 Recommendations

The methodology should be extended to other alkanes, such as pentane and methane. For methane, Ni and Pd catalysts should be synthesized and tested, and the experiment should be guided by phase equilibrium calculation to determine safe operating conditions.

To avoid the influence of phase separation on IR signal, the ReactIR probe could be fixed on the lateral surface of the reactor. In this case, the ReactIR could monitor the reaction solution even though there is phase separation or product precipitation on the bottom of the reactor.

Kinetic study of ozonolysis of cyclohexane in batch reactor will provide essential information for designing the continuous process. The determination of kinetic parameters will help in the rational reactor design and process development.

For reliable quantification of products, the calibration of various products from ozonolysis of isooctane should be done rigorously using response factors. For proper quantification of the formation of combustion products, the GC-MS method should be supplemented by Karl Fischer titration of the product mixture taking care to avoid moisture absorption from the atmosphere. The experimental studies must be complemented by computational reaction pathway analysis to better understand the reaction mechanism and the relative reactivities of the primary, secondary and tertiary carbons within the alkane. Such an understanding is essential for developing

rational strategies to promote selective formation of desired products during the ozonolysis of lighter alkanes.

References

[1] ""“Adipic acid (ADPA): 2014 world market outlook and forecast up to 2018” (Merchant Research and Consulting, Birmingham, UK, **2014**).".

[2] ""“Adipic acid (ADPA): 2018 world market outlook and forecast up to 2027” (Merchant Research and Consulting, Birmingham, UK, **2018**).".

[3] A. Castellan, J. C. J. Bart, and S. Cavallaro, "Industrial production and use of adipic acid," Catalysis Today, vol. 9, no. 3, pp. 237-254, **1991**.

[4] A. Chauvel and G. Lefebvre, Petrochemical Processes. Editions OPHRYS, **1989**.

[5] T. L. Brown, H. E. LeMay Jr, B. E. Bursten, and J. R. Burdge, Química. Pearson Educación, **2004.**

[6] J. Hoigne, "The Handbook of Environmental Chemistry Vol. 5, Part C, Quality and Treatment of Drinking Water II," ed: Springer-Verlag, **1998**.

[7] H. E. de Boer, C. M. van Elzelingen-Dekker, C. M. van Rheenen-Verberg, and L. Spanjaard, "Use of gaseous ozone for eradication of methicillin-resistant Staphylococcus aureus from the home environment of a colonized hospital employee," Infection Control & Hospital Epidemiology, vol. 27, no. 10, pp. 1120-1122, **2006**.

[8] G. Rotzoll, "Mass spectrometric investigation and computer modeling of the methane-oxygen-ozone reaction from 480 to 830 K," The Journal of Physical Chemistry, vol. 90, no. 4, pp. 677-683, **1986**.

[9] H. Gesser, N. Hunter, and P. Das, "The ozone sensitized oxidative conversion of methane to methanol and ethane to ethanol," Catalysis Letters, vol. 16, no. 1-2, pp. 217-221, **1992**.

[10] G. Zhu, H. Gesser, and N. Hunter, "The O_3 Sensitized Partial Oxidation of CH_4 to CH_3OH," in Studies in Surface Science and Catalysis, vol. 81: Elsevier, pp. 373-378, **1994**.

[11] C. K. Westbrook and F. L. Dryer, "Chemical kinetic modeling of hydrocarbon combustion," Progress in Energy and Combustion Science, vol. 10, no. 1, pp. 1-57, **1984**.

[12] A. Bozovic et al., "Conversion of methane to methanol: nickel, palladium, and platinum (d9) cations as catalysts for the oxidation of methane by ozone at room temperature," Chemistry- A European Journal, vol. 16, no. 38, pp. 11605-10, Oct 11 **2010**.

[13] "One-pot room-temperature conversion of cyclohexane to adipic acid by ozone and UV light," Science, vol 346, no. 6216, pp. 1495-1498, **2014**.

[14] B. Rindone, F. Saliu, and R. S. Bertoa, "Functionalization of the Unactivated Carbon-Hydrogen Bond Via Ozonation," Ozone: Science & Engineering, vol. 30, no. 2, pp. 165-171, **2008**.

[15] E. V. Avzyanova, Q. K. Timerghazin, A. F. Khalizov, S. L. Khursan, L. V. Spirikhin, and V. V. Shereshovets, "Formation of hydrotrioxides during ozonation of hydrocarbons on silica gel. Decomposition of hydrotrioxides," Journal of Physical Organic Chemistry, vol. 13, no. 2, pp. 87-96, **2000**.

[16] B. Barletta, E. Bolzacchini, L. Fossati, S. Meinardi, M. Orlandi, and B. Rindone, "Metal-free functionalization of the unactivated carbon-hydrogen bond: The oxidation of cycloalkanes to cycloalkanones with ozone," Ozone: Science & Engineering, **1998**.

[17] S. Rakovsky, M. Anachkov, V. Georgiev, A. Berlin, M. Belitski, and G. Zaikov, "Ozonation of Hydrocarbons," Research Progress in Chemical Physics and Biochemical Physics, p. 1. **2014**.

[18] C. Song, "Global challenges and strategies for control, conversion and utilization of CO_2 for sustainable development involving energy, catalysis, adsorption and chemical processing," Catalysis Today, vol. 115, no. 1-4, pp. 2-32, **2006**.

[19] M. Aresta and E. Quaranta, "Carbon dioxide: a substitute for phosgene," Chemtech, vol. 27, no. 3, **1997**.

[20] M. Aresta, "Perspectives of carbon dioxide utilisation in the synthesis of chemicals. Coupling chemistry with biotechnology," in Studies in Surface Science and Catalysis, vol. 114: Elsevier, pp. 65-76, **1998**.

[21] M. Aresta, "Key issues in carbon dioxide utilization as a building block for molecular organic compounds in the chemical industry," Preprints-American Chemical Society. Division of Petroleum Chemistry, vol. 45, no. 1, pp. 92-93, **2000**.

[22] M. Aresta ed., Carbon dioxide recovery and utilization. Springer Science & Business Media, **2013**.

[23] M. Aresta, "Carbon dioxide utilization: greening both the energy and chemical industry: an overview," in ACS Symposium Series, 2003, vol. 852, pp. 2-41: Washington, DC; American Chemical Society; **1999**.

[24] M. Aresta, A. Dibenedetto, and I. Tommasi, "Developing innovative synthetic technologies of industrial relevance based on carbon dioxide as raw material," Energy & Fuels, vol. 15, no. 2, pp. 269-273, **2001**.

[25] M. Aresta and A. Dibenedetto, "The contribution of the utilization option to reducing the CO_2 atmospheric loading: research needed to overcome existing barriers for a full exploitation of the potential of the CO_2 use," pp. 455-462, **2004**.

[26] T. Inui, M. Anpo, K. Izui, S. Yanagida, and T. Yamaguchi, eds. Advances in chemical conversions for mitigating carbon dioxide. Vol. 114. Elsevier, **1998**.

[27] T. Inui, "Effective conversion of CO_2 to valuable compounds by using multi-functional catalysts," Preprints-American Chemical Society. Division of Petroleum Chemistry, vol. 45, no. 1, pp. 113-117, **2000**.

[28] T. Inui and J. Spivey, Reforming of CH_4 by CO_2, O_2 and/or H_2O. Vol. 16. The Royal Society of Chemistry: London, **2002**.

[29] H. Arakawa, "Research and development on new synthetic routes for basic chemicals by catalytic hydrogenation of CO_2," in Studies in Surface Science and Catalysis, vol. 114: Elsevier, pp. 19-30, **1998**.

[30] S. Park, J. Yoo, K. Jun, D. Raju, J. Chang, and K. Lee, "Heterogeneous catalytic activation of carbon dioxide as an oxidant," Am. Chem. Soc. Div. Fuel Chem. Prepr., 46(1), 115-118, **2001**.

[31] J. Rostrup-Nielsen, "Aspects of CO_2-reforming of methane," in Studies in Surface Science and Catalysis, vol. 81: Elsevier, pp. 25-41, **1994**.

[32] J. Rostrup-Nielsen, J.-H. B. Hansen, and L. Aparicio, "Reforming of hydrocarbons into synthesis gas on supported metal catalysts," Journal of the Japan Petroleum Institute, vol. 40, no. 5, pp. 366-377, **1997**.

[33] S. Wang, G. Lu, and G. J. Millar, "Carbon dioxide reforming of methane to produce synthesis gas over metal-supported catalysts: state of the art," Energy & Fuels, vol. 10, no. 4, pp. 896-904, **1996**.

[34] M. Bradford and M. Vannice, "CO_2 reforming of CH_4," Catalysis Reviews, vol. 41, no. 1, pp. 1-42, **1999**.

[35] Y. H. Hu and E. Ruckenstein, "Catalytic conversion of methane to synthesis gas by partial oxidation and CO_2 reforming," ChemInform, vol. 35, no. 49, pp. no-no, **2004**.

[36] P. G. Jessop, T. Ikariya, and R. Noyori, "Homogeneous catalysis in supercritical fluids," Science, vol. 269, no. 5227, pp. 1065-1069, **1995**.

[37] P. G. Jessop, T. Ikariya, and R. Noyori, "Homogeneous hydrogenation of carbon dioxide," Chemical Reviews, vol. 95, no. 2, pp. 259-272, **1995**.

[38] P. G. Jessop, F. Joó, and C.-C. Tai, "Recent advances in the homogeneous hydrogenation of carbon dioxide," Coordination Chemistry Reviews, vol. 248, no. 21-24, pp. 2425-2442, **2004**.

[39] W. Leitner, "Reactions in supercritical carbon dioxide ($scCO_2$)," in Modern Solvents in Organic Synthesis: Springer, pp. 107-132, **1999**.

[40] A. I. Cooper, "Polymer synthesis and processing using supercritical carbon dioxide," Journal of Materials Chemistry, vol. 10, no. 2, pp. 207-234, **2000**.

[41] R. S. Oakes, A. A. Clifford, and C. M. Rayner, "The use of supercritical fluids in synthetic organic chemistry," Journal of the Chemical Society, Perkin Transactions 1, no. 9, pp. 917-941, **2001**.

[42] G. Musie, M. Wei, B. Subramaniam, and D. H. Busch, "Catalytic oxidations in carbon dioxide-based reaction media, including novel CO_2-expanded phases," Coordination Chemistry Reviews, vol. 219, pp. 789-820, **2001**.

[43] B. Subramaniam and D. H. Busch, "Use of Dense-Phase Carbon Dioxide in Catalysis," in: C.S. Song, A. M. Gaffney, K. Fujimoto (Eds.), CO_2 Conversion and Utilization, American Chemical Society, Washington DC, ACS Symposium Series, vol. 809, pp. 364–386 (Chapter 24), **2002**.

[44] M. D. Lundin, A. M. Danby, G. R. Akien, T. P. Binder, D. H. Busch, and B. Subramaniam, "Liquid CO_2 as a Safe and Benign Solvent for the Ozonolysis of Fatty Acid Methyl Esters," ACS Sustainable Chemistry & Engineering, vol. 3, no. 12, pp. 3307-3314, **2015**.

[45] M. D. Lundin et al., "Intensified and safe ozonolysis of fatty acid methyl esters in liquid CO_2 in a continuous reactor," AIChE Journal, **2017**.

[46] M. G. Zabetakis, "Flammability characteristics of combustible gases and vapors," No. BULL-627, Bureau of Mines Washington DC, **1965**.

[47] G.-I. Kaminishi, C. Yokoyama, and T. Shinji, "Vapor pressures of binary mixtures of carbon dioxide with benzene, n-hexane and cyclohexane up to 7 MPa," Fluid Phase Equilibria, vol. 34, no. 1, pp. 83-99, **1987**.

[48] A. Fredenslund and G. Sather, "Gas-liquid equilibrium of the oxygen-carbon dioxide system," Journal of Chemical and Engineering Data, vol. 15, no. 1, pp. 17-22, **1970**.

[49] E. Wilhelm and R. Battino, "The solubility of gases in liquids. 5. The solubility of N_2, O_2, CO, and CO_2 in cyclohexane at 283 to 313 K," The Journal of Chemical Thermodynamics, vol. 5, no. 1, pp. 117-120, **1973**.

[50] H. F. Coward and G. W. Jones, "Limits of flammability of gases and vapors," No. BM-BULL-503., Bureau of Mines Washington DC, **1952**.

[51] D. A. Crowl, Understanding explosions. Vol. 16, John Wiley & Sons, **2010**.

[52] P. J. Hesse, R. Battino, P. Scharlin, and E. Wilhelm, "Solubility of gases in liquids. 21. Solubility of He, Ne, Ar, Kr, N_2, O_2, CH_4, CF_4, and SF_6 in 2, 2, 4-trimethylpentane at T= 298.15 K," The Journal of Chemical Thermodynamics, vol. 31, no. 9, pp. 1175-1181, **1999**.

[53] F. Mutelet, S. Vitu, R. Privat, and J.-N. Jaubert, "Solubility of CO_2 in branched alkanes in order to extend the PPR78 model (predictive 1978, Peng–Robinson EOS with temperature-

dependent k ij calculated through a group contribution method) to such systems," Fluid phase equilibria, vol. 238, no. 2, pp. 157-168, **2005**.

Appendix

1. Cyclohexanol and Cyclohexanone Stayed in Liquid Phase during Reaction.

Table A-1: Gas phase hydrocarbons detected during ozonolysis of cyclohexane.

	Gas phase hydrocarbons collected in various runs (mol)	
Cyclohexane conversion (%)	22.9	18
Cyclohexane (mol)	6.7 (10^{-4}) (9.3%)	1.2 (10^{-3}) (16%)
Cyclohexanone (mol)	9.5 (10^{-6})	1.8 (10^{-5})
Cyclohexanol (mol)	Not detected	Not detected

*Reaction conditions: 9.22×10^{-3} mol cyclohexane, O_3/cyclohexane = 49-51%. 280 K, 6.7 MPa, 400 rpm, 1 hr). The number in the parentheses are the percentage of gaseous cyclohexane in total cyclohexane (liquid + gas phases).

2. Confirmation of Cyclohexanone and Cyclohexanol Formation by GC-MS Method.

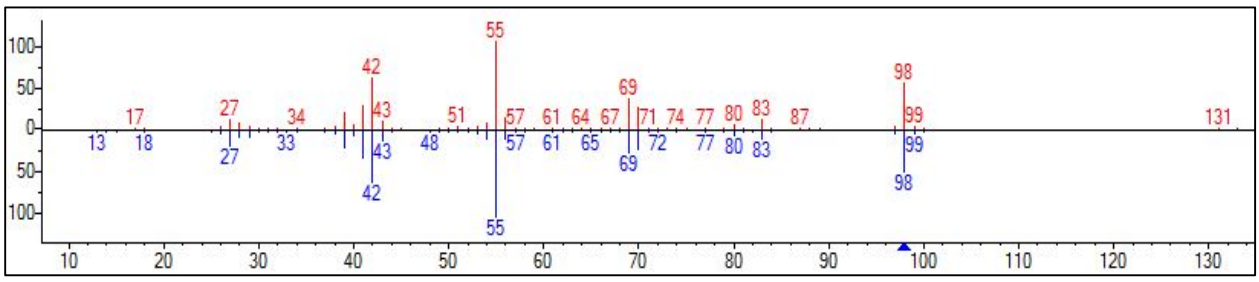

Figure A-1: Mass fragmentation pattern of cyclohexanone by GC-MS method.

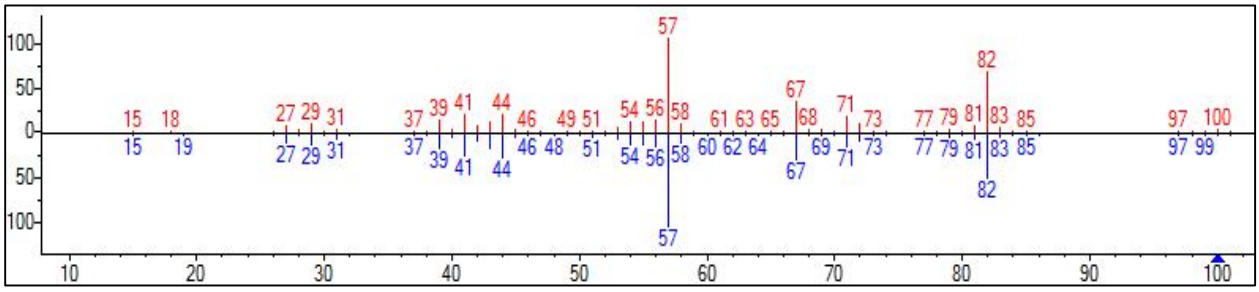

Figure A-2: Mass fragmentation pattern of cyclohexanol by GC-MS method.

3. Calibration of Concentrations of Cyclohexane and Products.

3.1 Calibration using Organic Solvents by ReactIR.

The calibrations for the concentrations of cyclohexane, cyclohexanone and cyclohexanol by ReactIR 15 were carried out using IR absorbance peaks at wavenumbers of 2857 cm^{-1}, 1723 cm^{-1} and 1067 cm^{-1}, respectively. The infrared absorbance for each component is shown in Figure A-3. Since there is no IR spectrum overlapping between toluene and cyclohexane at 2857 cm^{-1} (see Figure A-4), toluene was used as solvent for the calibration of cyclohexane concentrations in ReactIR. Same principle for solvent selection was applied to the calibration of cyclohexanone (see Figure A-5) and cyclohexanol (see Figure A-6) concentrations. Standard solutions for each product were prepared in volumetric flasks separately, with their IR spectra recorded at 293 K, 0.1 MPa. The concentrations of standard solutions for each component and their IR absorbance (as of A.U.) were combined to plot the calibration figure. See results in Figure A-7, A-8, A-9.

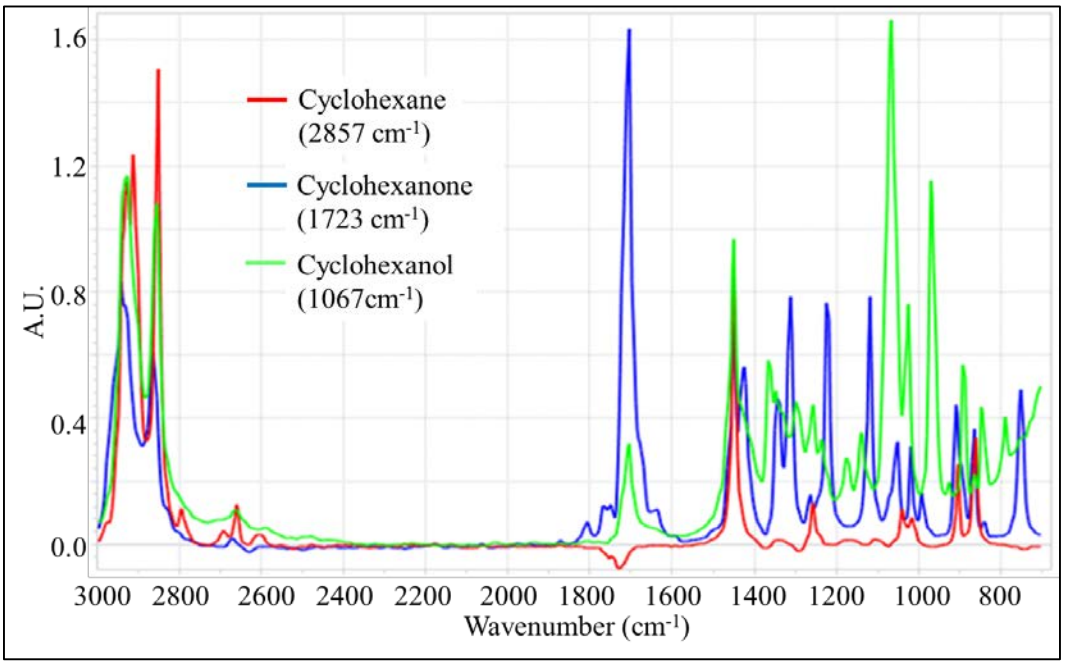

Figure A-3: IR spectra of cyclohexane, cyclohexanone and cyclohexanol.

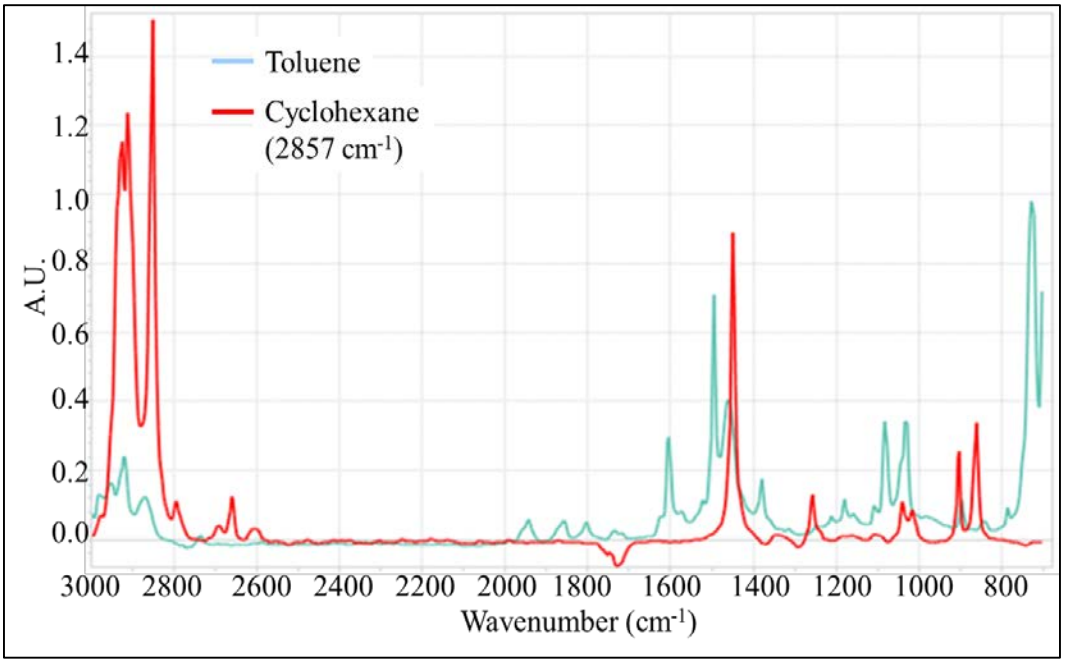

Figure A-4: IR spectra of cyclohexane and toluene.

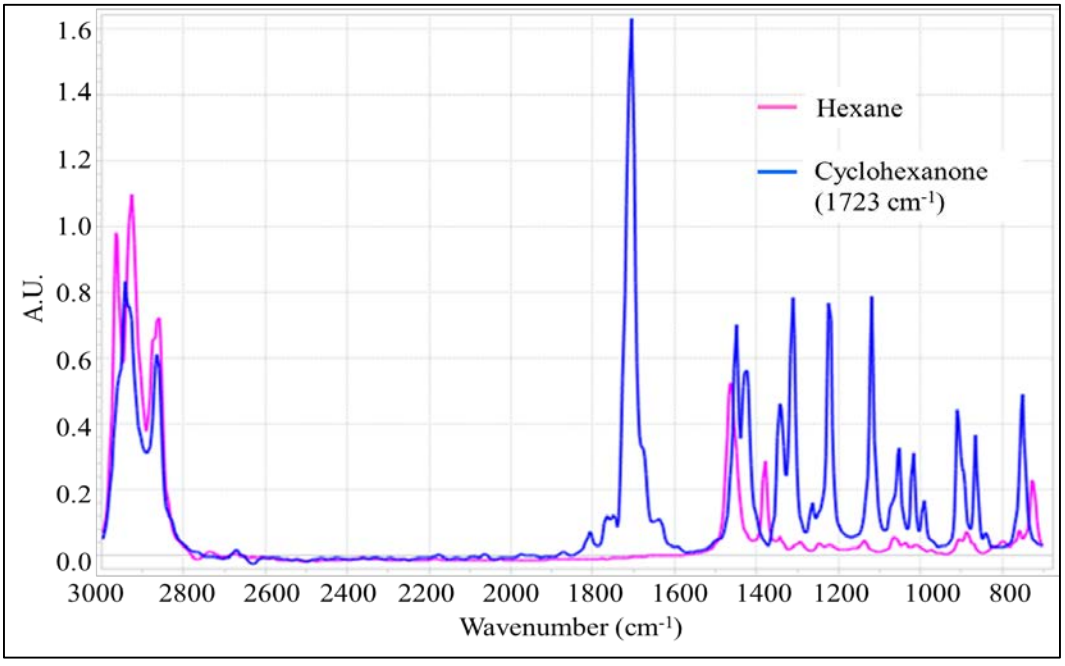

Figure A-5: IR spectra of cyclohexanone and hexane.

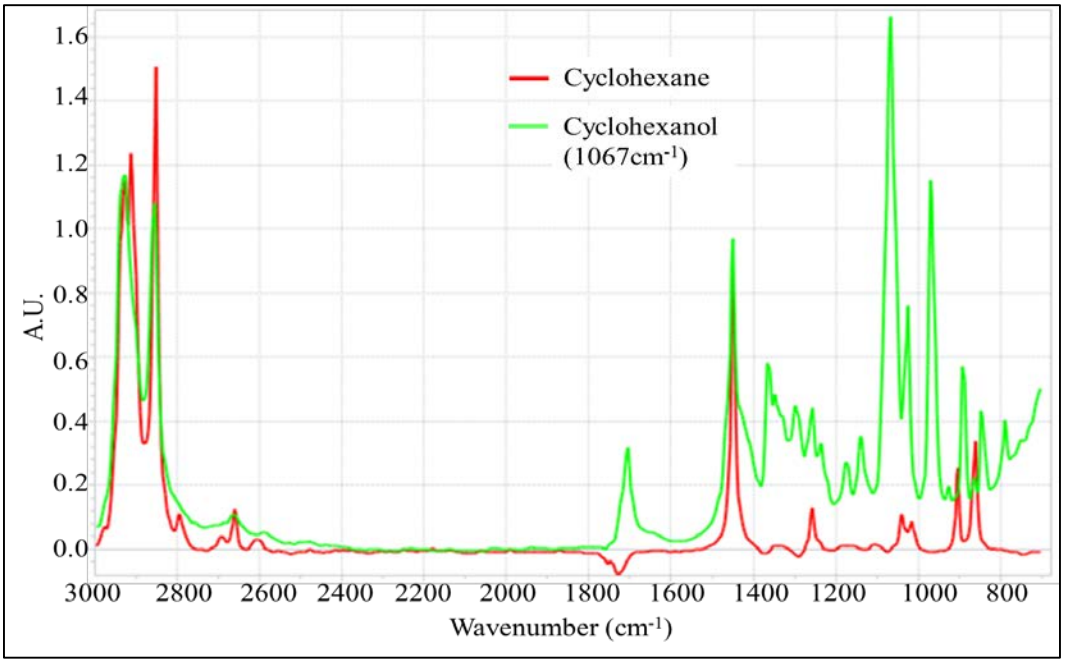

Figure A-6: IR spectra of cyclohexanol and cyclohexane.

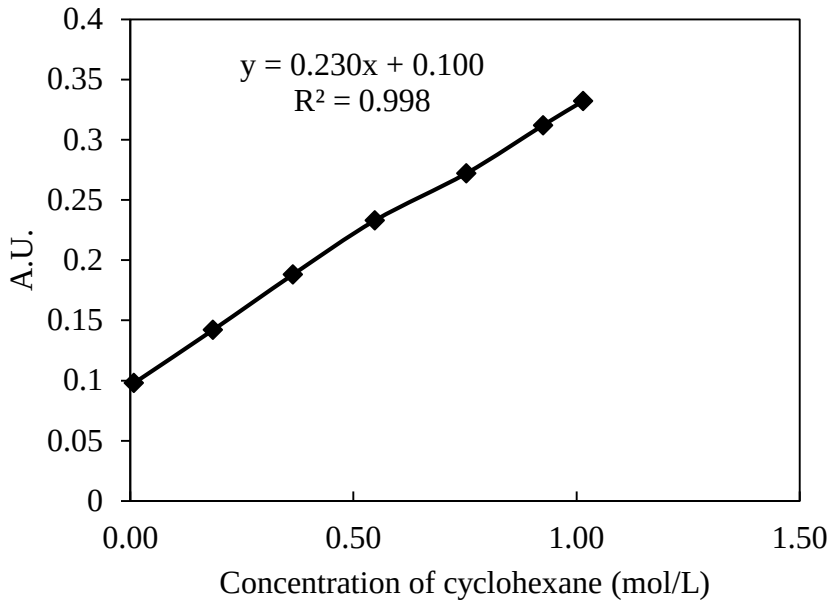

Figure A-7: Calibration of concentrations of cyclohexane in toluene by ReactIR.

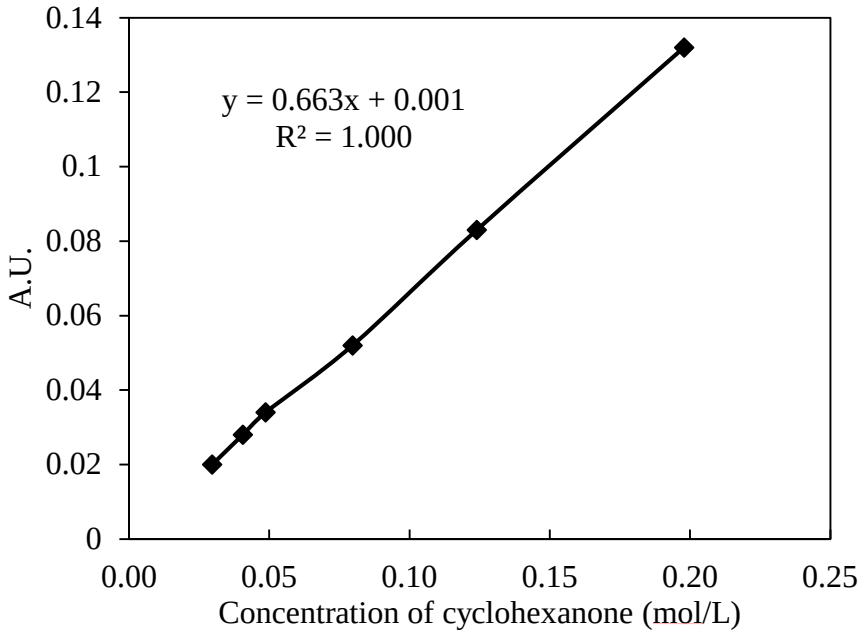

Figure A-8: Calibration of concentrations of cyclohexanone in hexane by ReactIR.

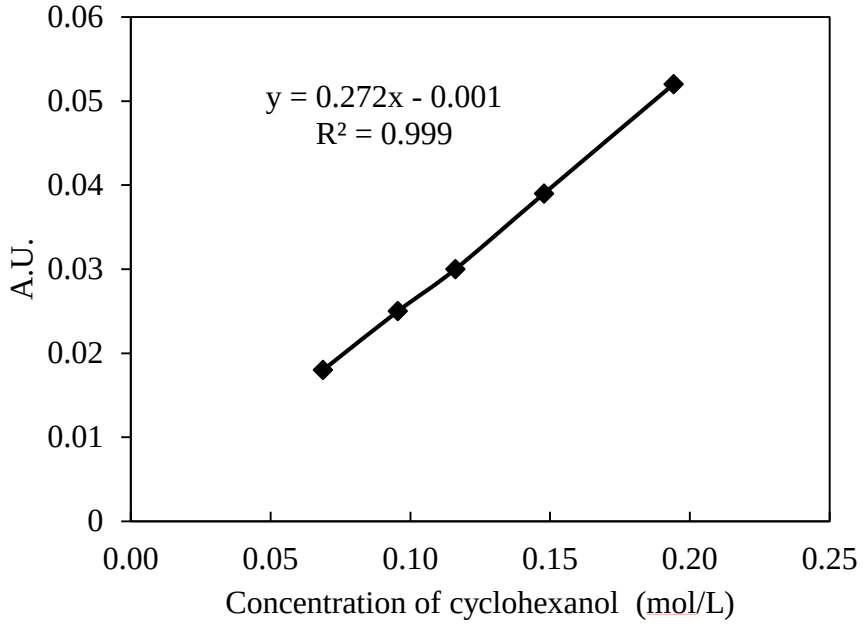

Figure A-9: Calibration of concentrations of cyclohexanol in cyclohexane by ReactIR.

3.2 Calibration of Concentrations of Cyclohexane in Liquid CO_2 by ReactIR.

The calibration of concentrations of cyclohexane in liquid CO_2 was performed using ReactIR. The IR absorbance peak of cyclohexane at 2939 cm^{-1} was chosen for calibration as shown in Figure A-10. Certain amount of CO_2 in ISCO pump (3.64 MPa, 293 K, 266 mL) was fed into reactor where it then reached equilibrium at 280 K, 4.14 MPa. The liquid CO_2 formed at this condition was scanned and taken as IR background by ReactIR 10. Next, liquid cyclohexane was pumped into the reactor by ISCO pump at 293 K, and the binary mixture was stirred at 400 rpm to reach equilibrium followed by IR scan and recording. The flow rate of ISCO pump was set at 1.5 $mL \cdot min^{-1}$. The quantity of cyclohexane pumped into the reactor was controlled by the pumping time. The density of CO_2 and cyclohexane at these conditions were retrieved from NIST database SRD 69 to give an accurate calculation. The VLE of cyclohexane and CO_2 binary system was modelled by Aspen Plus using Peng- Robinson EOS, with the concentrations of cyclohexane in liquid phase calculated and applied to plot the calibration figure. Figure A-11 shows the calibration result.

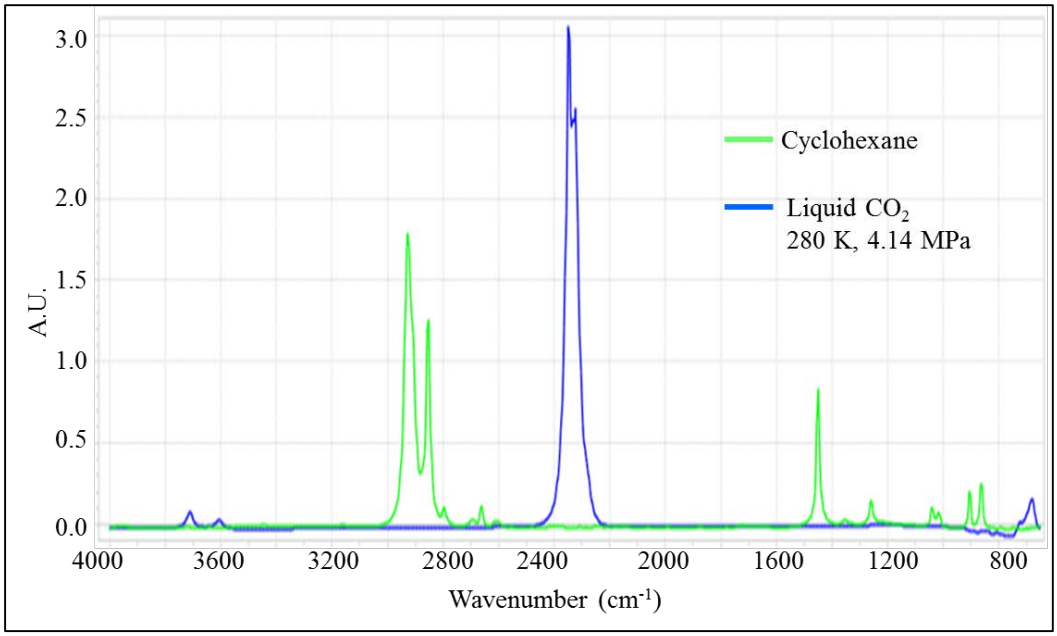

Figure A-10: IR spectra of cyclohexane and liquid CO_2 (280 K, 4.14 MPa).

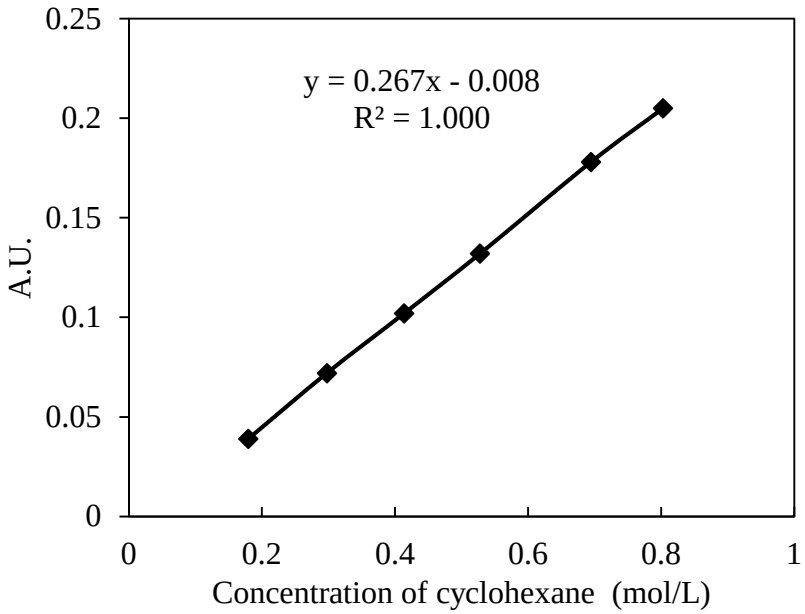

Figure A-11: Calibration of concentrations of cyclohexane in liquid CO_2 (280 K, 4.14 MPa) by ReactIR.

3.3 Calibration by GC-FID.

To calculate the conversion and selectivity by GC-FID method, a series of standard solutions of cyclohexane, cyclohexanol and cyclohexanone in acetone were prepared in a volumetric flask at room temperature and were analyzed by the GC-FID method. The concentrations of standard solutions and each component's peak area in the FID chromatogram were integrated to plot the calibration figure. Figure A-12, A-13 and A-14 show the results.

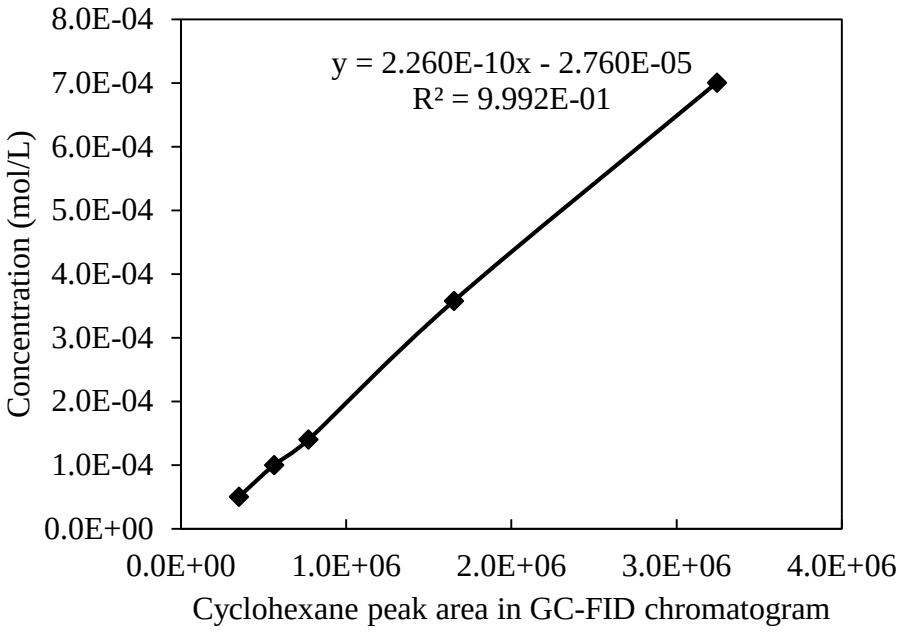

Figure A-12: Calibration of concentrations of cyclohexane in acetone by GC-FID.

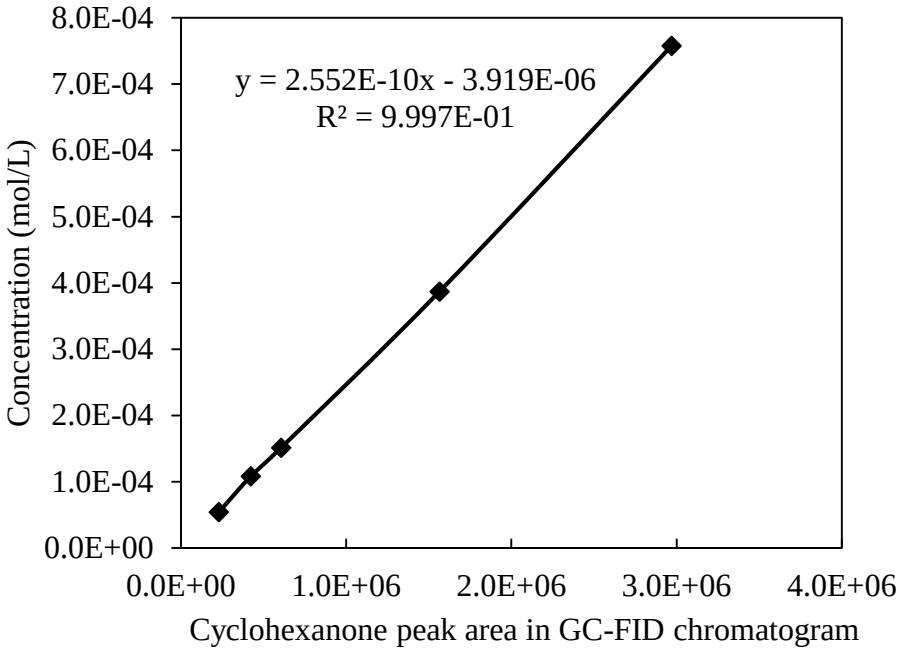

Figure A-13: Calibration of concentrations of cyclohexanone in acetone by GC-FID.

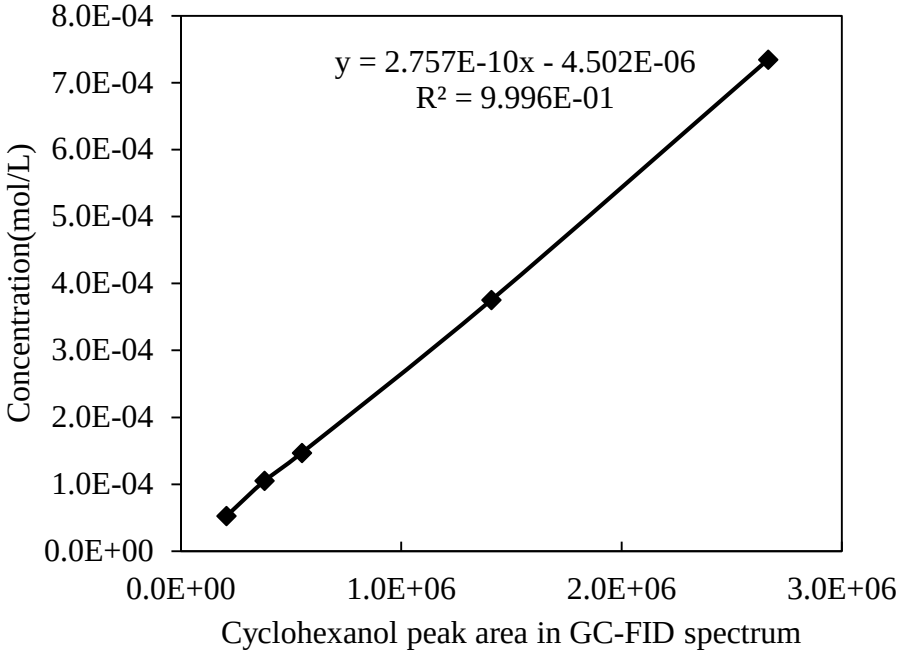

Figure A-14: Calibration of concentrations of cyclohexanol in acetone by GC-FID.

4. Minor Products from Ozonolysis of Cyclohexane.

Table A-2: Distribution of minor products from ozonolysis of cyclohexane.

1mL cyclohexane, ozone: cyclohexane = 48.6%, 280 K, 6.7 MPa, 400 rpm, 1 hr				
Products	Peak Area Counts in GC-FID Chromatogram	Total Area	Area Ratio to Cyclohexane[a]	Yield [b]
Acetic acid	1071372	9.12E+06	1:100 (1%)	0.80 mol%
Oxalic acid	191981			
Butyrolactone	288999			
Pentanoic acid	194451			
Tetrahydro-2-pyranone	598308			
Hexanoic acid	118531			
1,4-cyclohexanedione	754383			
Succinic anhydride	73849			
Propanoic acid	494363			
Butanoic acid	1162297			
Heptanoic acid	2368298			
Hexanoic acid, 6-hydroxy-	774322			
Butanal, 3-hydroxy-	173771			
2-Oxepanone	313330			
Cyclohexanone, 2-hydroxy-	134870			
Cyclohexanone,4-hydroxy-	135655			
Cyclohexanone,3-hydroxy-	273334			

[a] Area Ratio to Cyclohexane: total area of minor products / area of cyclohexane in products' FID chromatogram; [b] Yield = moles of minor products / initial moles of cyclohexane.

5. Mass Fragmentation Patterns of Products from Ozonolysis of Iso-octane.

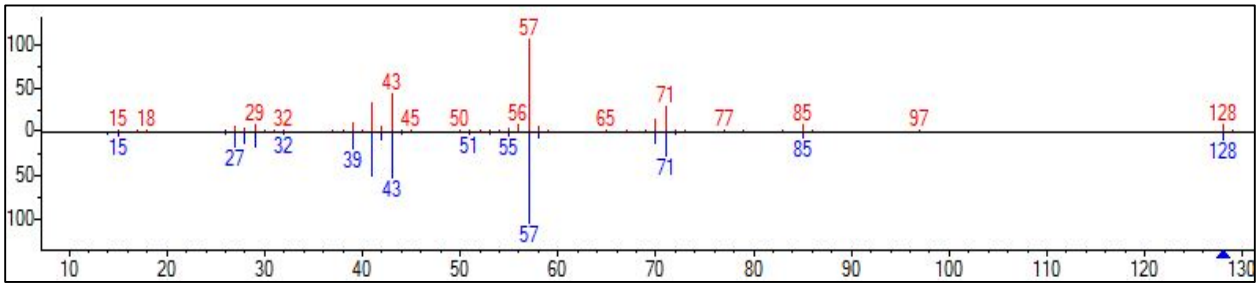

Figure A-15: Mass fragmentation pattern of 2,2,4-trimethyl-pentanone by GC-MS.

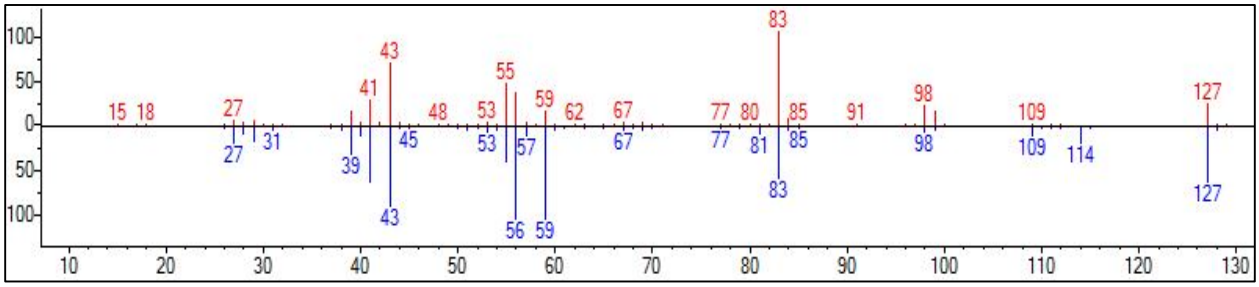

Figure A-16: Mass fragmentation pattern of 3,3,5,5-tetramethylbutyrolactone by GC-MS.

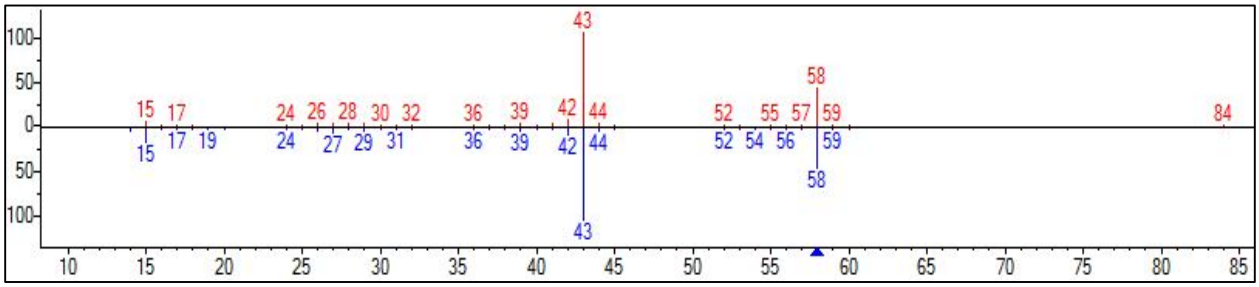

Figure A-17: Mass fragmentation pattern of acetone by GC-MS.

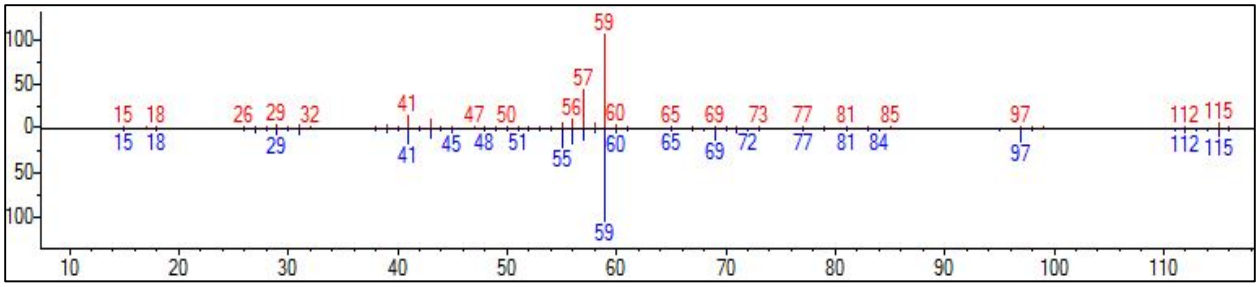

Figure A-18: Mass fragmentation pattern of 2,4,4-trimethyl-2-pentanol by GC-MS.

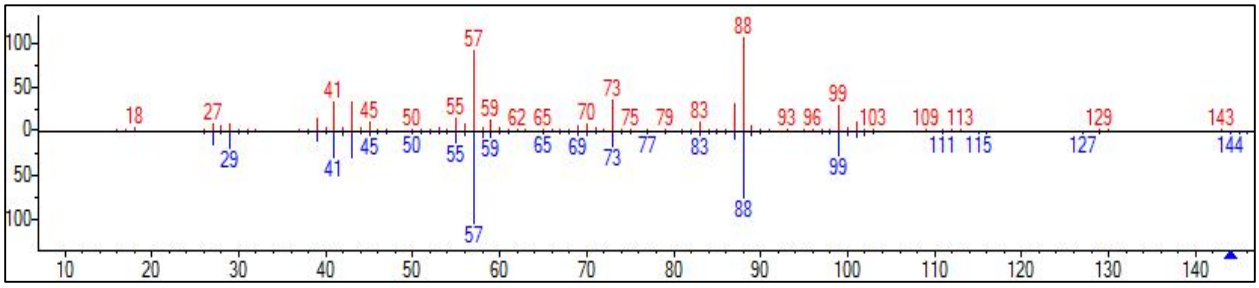

Figure A-19: Mass fragmentation pattern of 2,2,4-trimethylpentanoic acid by GC-MS.

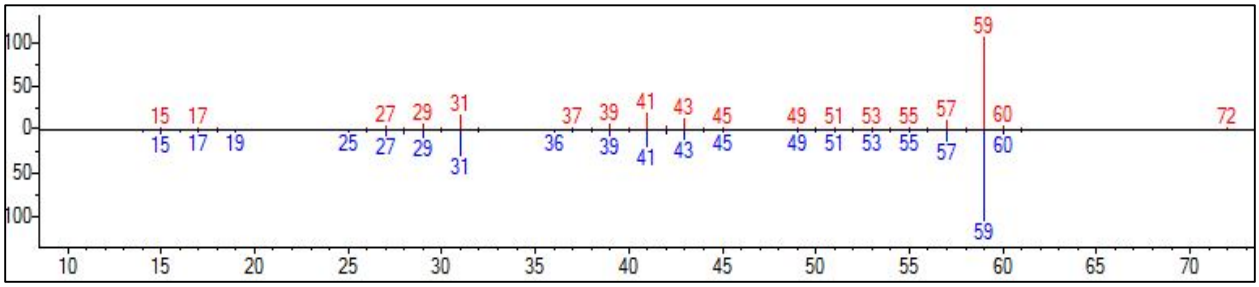

Figure A-20: Mass fragmentation pattern of tert-butyl alcohol by GC-MS.

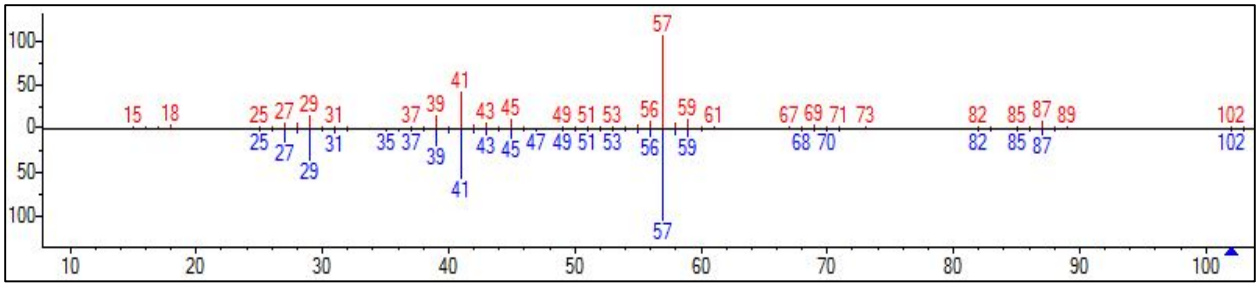

Figure A-21: Mass fragmentation pattern of pivalic acid by GC-MS.

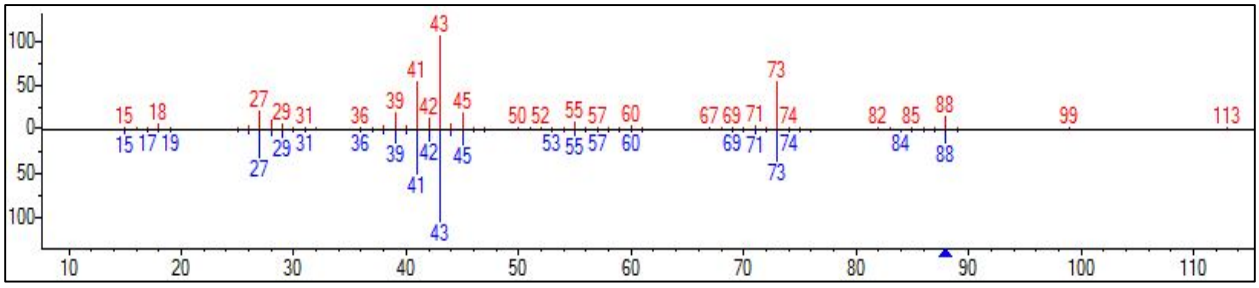

Figure A-22: Mass fragmentation pattern of isobutyric acid by GC-MS.

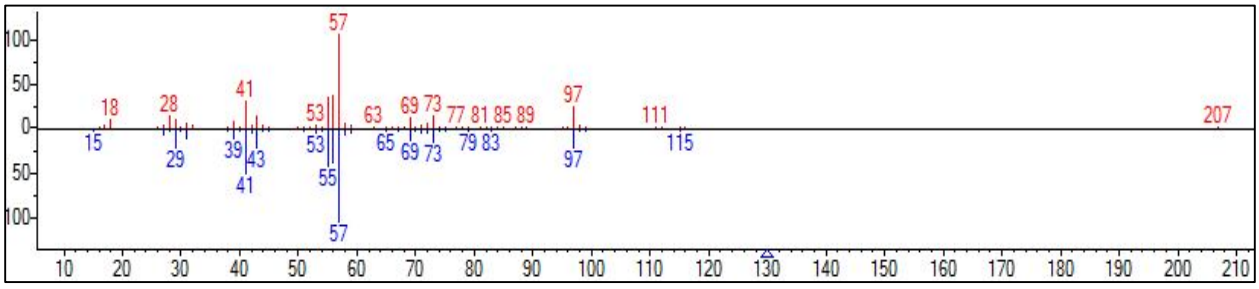

Figure A-23: Mass fragmentation pattern of 2,4,4-trimethyl-1-pentanol by GC-MS.

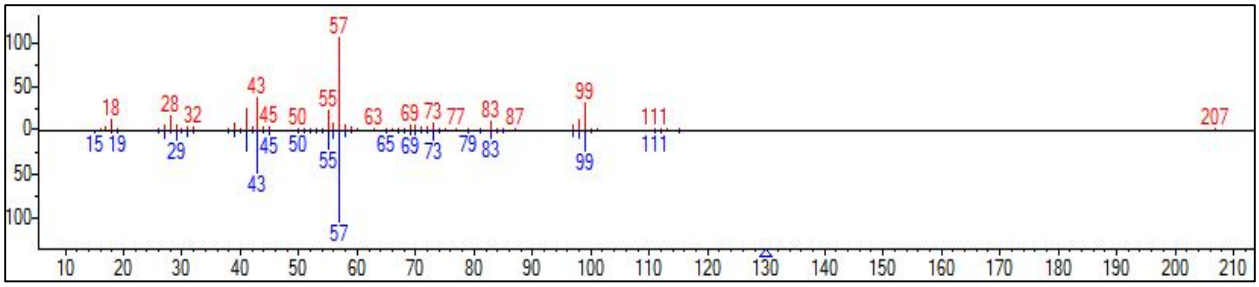

Figure A-24: Mass fragmentation pattern of 2,2,4-trimethyl-1-pentanol by GC-MS.

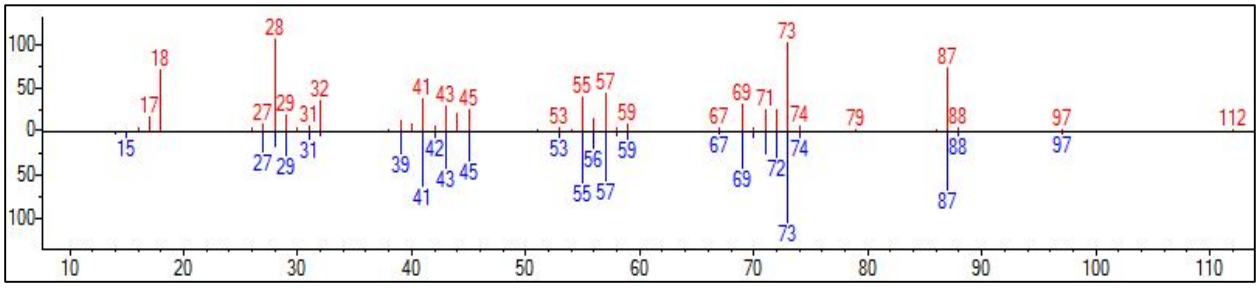

Figure A-25: Mass fragmentation pattern of 2,2,4-trimethyl-3-pentanol by GC-MS.

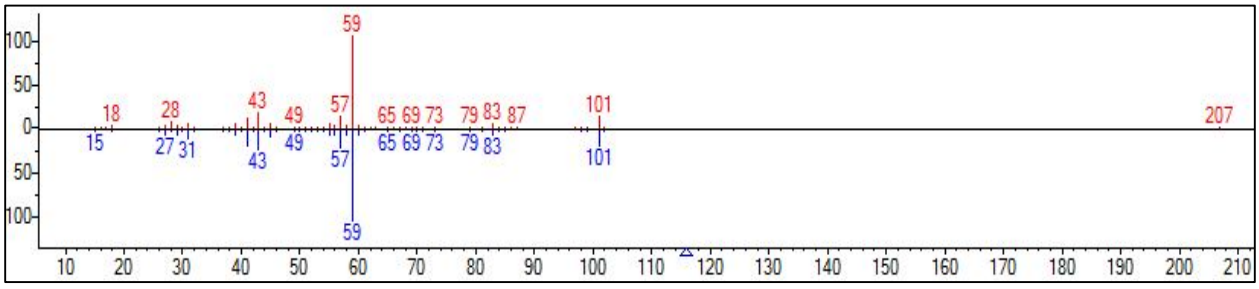

Figure A-26: Mass fragmentation pattern of 2,4-dimethyl-2-pentanol by GC-MS.

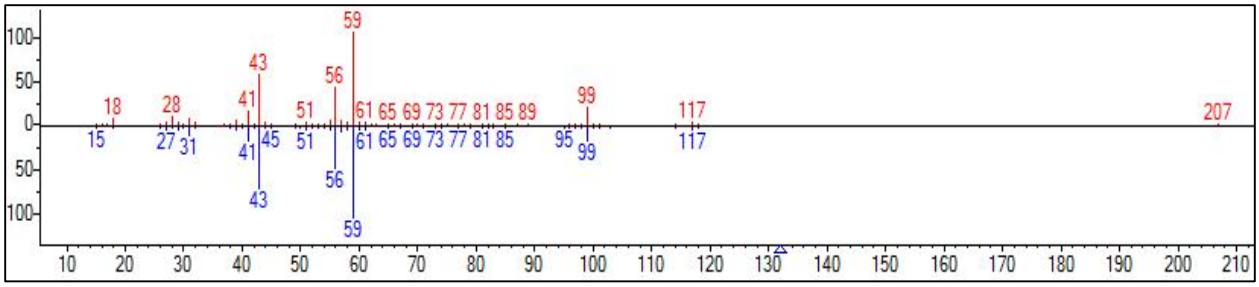

Figure A-27: Mass fragmentation pattern of 2,4-dimethyl-2,4-pentanediol by GC-MS.

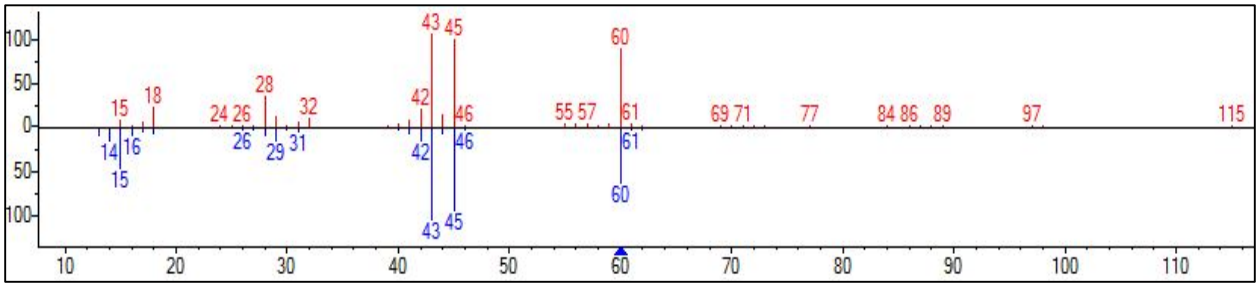

Figure A-28: Mass fragmentation pattern of acetic acid by GC-MS.